

ABSTRACT

Title of Dissertation: Novel Adaptations in Morphology, Development, and Nutrient Acquisition for Host Exploitation in the Mesostigmatid Honey Bee Parasite *Varroa destructor*

Samuel Ramsey, Doctor of Philosophy, 2018

Dissertation directed by: Assistant Professor, Dennis vanEngelsdorp, Entomology Department

The parasitic mite *Varroa destructor* is the most significant single driver of the global honey bee health decline. Better understanding of the association of this parasite and its host is critical to developing sustainable management practices. This work shows that *Varroa* is not consuming hemolymph as has been the accepted view, but damages host bees by consuming fat body. Feeding wounds in adult bees were imaged for the first time showing that *Varroa* feed on the underside of the abdomen where fat body is the immediate underlying tissue. Fat body at the wound site showed evidence of external digestion. Hemolymph and fat body in honey bees were then marked with fluorescent biostains. Fluorescence associated with the fat body was consistently detected in the gut of mites fed on these bees while comparatively little fluorescence was detected from the hemolymph biostain. Mites were then fed a diet composed of one or both tissues. Mites fed fat body tissue survived longer and produced more eggs than those fed hemolymph. Mites fed hemolymph showed fitness metrics no different from the starved control group. Collectively, these findings show that *Varroa* are exploiting the fat body as their primary source of sustenance; a tissue integral to proper immune function, pesticide detoxification, overwinter survival and several other essential processes in healthy adult and immature bees. Additional study was undertaken to better understand how the *Varroa* accelerates its reproductive rate. Via gel electrophoresis and immunodetection, undigested honey bee vitellogenin was found in *Varroa* eggs. The presence and identity of these host proteins was confirmed via HPLC MS/MS. This particular cleavage of vitellogenin is found only in the fat body. These findings fundamentally alter our understanding of the etiology of varroosis and underscore a need to revisit our understanding of this parasite and its impacts, both direct and indirect, on honey bee health. Further study of *Varroa* adaptations focused on expanding knowledge of *Varroa* morphology with the aim of determining features that can distinguish between *Varroa* species. Using low temperature scanning electron microscopy, we were able to provide better resolution of key morphological features, detail variability within traits, and provide novel descriptions of certain characters.

NOVEL ADAPTATIONS IN MORPHOLOGY, DEVELOPMENT, AND
NUTRIENT ACQUISITION FOR HOST EXPLOITATION IN THE
MESOSTIGMATID HONEY BEE PARASITE *VARROA DESTRUCTOR*

by

Samuel David Ramsey

Dissertation submitted to the Faculty of the Graduate School of the
University of Maryland, College Park, in partial fulfillment
of the requirements for the degree of
Doctor of Philosophy
2018

Advisory Committee:

Professor Dennis vanEngelsdorp, Chair

Pedro Barbosa

Jay Evans

Cerrutti Hooks

John Lea-Cox

Ronald Ochoa

© Copyright by
Samuel David Ramsey
2018

Preface

Symbiosis is among the most fascinating and convoluted phenomena in science. However, this term is often used as if it encompasses only mutualistic interactions between organisms ignoring the captivating and ecologically salient interactions defined broadly as parasitism. It is already an impressive feat to make a meal of a creature that does not wish to be food but to adapt one's self to live on or in that unwilling food resource is that much more of an exploit. This lifecycle has such distinct benefits that it is seen in some of the earliest lifeforms on the planet. It involves such unrelenting evolutionary pressure that it demands ever more extreme adaptation. Lifecycles may involve behavioral manipulation, castration, resource thievery, chemical mimicry, biological warfare, sacrificial siblings, induction of tumors or superfluous limbs, secondary, tertiary, or even quaternary parasitism, amputation and replacement of a body part, or something akin to induced zombification. Researchers have suggested that there may well be a parasite of every single insect species with many being species specific parasites of insect eggs. The heterogeneity evinced in these relationships is truly astonishing; diversity of a level that I hope one day is reflected in the researchers studying this riveting facet of the sciences.

Dedication

This work is dedicated with love to my parents, both my biological, Roosevelt and Sharon Ramsey, and my non-biological, though no less significant parents, Dr. Kevin and Kathy Hackett. Further, my siblings Ashley and Immanuel Ramsey share in this achievement as some of the first minds to have molded mine and I would like to dedicate this work to them as well.

Acknowledgments

I am grateful to Karen Rennich, Dan Reynolds, Heather Eversole, and Rachel Fahey for technical support, equipment procurement, and just generally their friendly reliability. I could not have done this without all of their help. I am also grateful to Nathalie Steinhauer for statistical advice and support, Todd Waters for figure illustration, and Andrew Garavito for beekeeping advice and maintenance of the University of Maryland Apiaries. In addition, I appreciate the help of Andrew Ulsamer with technical support, Chris Pooley with image processing, Jim Zastrow and Zastrow Services for building custom equipment for this project, as well as Dr. Carlton Green, Dean Jeff Franke, and Sue Wecht for great advice and exceptionally well-timed morale boosts. I would also like to acknowledge the contributions and friendship of former committee member Dr. Bahram Momen; a great researcher who we lost far too early. I would like to thank the University of Maryland, Department of Entomology; Smithsonian Natural History Museum, Soybean Genomics & Improvement Laboratory, Systematic Entomology Laboratory and the USDA ARS for their assistance with references, material and equipment for this study. This study was supported jointly by a grant from Project *Apis m.* and the Jackie Robinson Foundation. Finally, I would like to acknowledge Dr. Kumea Shorter-Gooden for her advice and advocacy without which, I likely would not have been able to complete my degree progress. No man is an island. Thank you all for that reminder.

Table of Contents

Preface.....	ii
Dedication.....	iii
Acknowledgements.....	iiv
Table of Contents.....	v
List of Tables.....	vii
List of Figures.....	viii
General Introduction:.....	1
Chapter 1: Determining the Feeding Site of <i>Varroa destructor</i> on Adult Honey Bees: Is There Actually a Phoretic Phase.....	3
Introduction.....	3
Methods.....	7
Determining Spatial Distribution of Apparently Feeding Mites.....	7
Transmission Electron Microscopy & Light Microscopy	7
Methods: Low-Temperature Scanning Electron Microscopy.....	8
Results.....	9
Discussion.....	14
Chapter 2: Identification of Host Tissue Consumed by <i>Varroa destructor</i> using Tissue Specific Fluorescent Biostains.....	17
Introduction.....	17
Methods.....	17
Tissue Biostain.....	17
Axiozoom Fluorescent Microscopy.....	21
Confocal Laser Scanning Microscopy	22
Results.....	22
Discussion.....	25
Chapter 3: Determination of the Suitability of a Honey Bee Hemolymph or Fat Body Diet for Survivorship and Reproduction of <i>Varroa destructor</i>.....	28
Introduction.....	28
Methods.....	28
Results.....	31
Discussion.....	32
Chapter 4: Reproductive Protein Stealing in <i>Varroa destructor</i>.....	36
Introduction.....	36
Methods.....	38
Sample Collection.....	38
Protein Separation and Identification.....	39
Vitellogenin Confirmation via HPLC MS/MS	40
Results.....	41
Protein Separation via Gel Electrophoresis	41
Vitellogenin Identification via Western Blot.....	41
Vitellogenin Confirmation via HPLC MS/MS	42
Discussion.....	44

Chapter 5: Morphology of <i>Varroa destructor</i> Detailed via Low-Temperature Electron Microscopy with Emphasis on Variable Characters	47
Introduction.....	47
Methods.....	50
Results.....	52
Peritremes	53
Ventral Sclerites.....	57
Gnathosoma	60
Legs.....	67
Peritremes	72
Interscutellar Membrane	72
Discussion.....	75
General Conclusion:.....	79
Appendices	82
Bibliography.....	83

List of Tables

Table 1

81

Table 1 detailing the nine primary functions of the fat body and related pathologies associated with *Varroa* feeding. Note that *Varroa* feeding negatively impacts each of the fat body functions.

List of Figures

Figure 1.1

11

Figure 1.1 *Varroa destructor* shows consistent preference for the underside of the metasoma of adult host bees, an area predominated by fat body tissue just beneath the cuticle.

a, Diagram showing frequency of dispersing *Varroa* found in each location on 104 parasitized worker bees in five trials (tg=tergite, st=sternite). *Varroa* were found on the underside of metasoma as opposed to locations on the mesosoma or head (GLM): $\chi^2 = 6.5$, $P < 0.001$. Mites strongly preferred the third segment of the metasoma to any of the other 23 locations (GLM: $\chi^2 = 4.5$, $P < 0.001$). Mites were also found preferentially on the left side of the host (Chi): $\chi^2 = 24.02$, $P < 0.001$.

Figure 1.2

12

Figure 1.2 Feeding site of *Varroa* in dispersal phase imaged on adult honey bee via Low Temperature Scanning Electron Microscopy (LT-SEM).

a-e, Colorized image of a worker bee parasitized by *Varroa* (white arrow) (**a** & **b**). The mite is wedged beneath the third tergite of the metasoma. When removed, a wound can be observed (**c**, **d**) matching the modified chelicera of the mite mouthparts (**e**). Image **c** colorized to show the impression of the mite left in the soft tissue of the bee.

f, Freeze fracture image showing a cross section of a mite at feeding site; note the thin intersegmental membrane (white arrow) and fat body and muscle tissue just on the other side. In the process of creating the fracture, the mite (black asterisk) was pushed away from the membrane.

Figure 1.3

13

Figure 1.3 Dispersing *Varroa* attached to worker bees were used to pinpoint the precise location of the feeding site, revealing the ultrastructural morphology of the feeding site wound, bacteria at the feeding site, and details of the fat body.

a,b, Histological cross section of a worker bee with *Varroa* attached in the feeding position at the third metasomal segment, arrows showing position of the fat body tissue lying directly beneath the intersegmental membrane (**a**). The feeding site wound in the membrane of the bee is clearly visible as a large mound with a hole intersecting the membrane, arrow indicating the hole (**b**).

c-e Transmission electron microscopy (TEM) images of the feeding site wound in the intersegmental membrane of the bee, showing a hole with irregular edges where the chelicera of the mite have penetrated the membrane. The black arrow indicates bacteria at the feeding site beneath the intersegmental membrane, and the white arrow indicates degraded fat body cells likely due to the extra-oral digestion. (**c**) Higher magnification reveals two species of morphologically distinct bacteria (**d**) and greater detail of irregularly shaped cell contents of the degraded fat body tissue (**e**).

f, TEM image of the fat body tissue showing a trophocyte with numerous vacuoles filled with electron dense lipid globules and an irregularly shaped nucleus.

Figure 2.1

24

Figure 2.1 Host tissue collected from bees with fluorescently stained internal tissues showing the fidelity of each biostain (Nile Red and Uranine) for each host tissue (fat body and hemolymph respectively).

a-d, Hemolymph tissue shown in brightfield (**a**), and with fluorescent imaging (**b**). Fat body tissue shown in brightfield (**c**), and with fluorescent imaging (**d**).

Figure 2.2

24

Figure 2.2 *Varroa* fed on nurse bees with fluorescently stained hemolymph and fat body tissue primarily showed fluorescence associated with fat tissue.

a,b, *Varroa* after having innate fluorescence (autofluorescence) of the integument reduced via hydrogen peroxide bath (**a**). Bright red fluorescence (associated with fat body biostain) can clearly be observed in its multi-lobed digestive system without dissection (**b**). Note, fluorescence associated with the hemolymph (yellow) is very low and virtually indiscernible when imaged.

c,d,e, Confocal microscopy images of dissected *Varroa* fed only one of the fluorescent biostains. Mites fed on bees with fluorescently stained fat body show such high levels of Nile Red in the digestive system that the shape of the gut can be clearly observed via fluorescence imaging. Mites that fed exclusively on bees with biostained hemolymph (**d**) showed fluorescence only marginally above the control (**e**).

Figure 2.3

24

Figure 2.3 Mean biostain levels detected in *Varroa* and in biostain honey bee tissues. Fluorescence values reported in arbitrary fluorescence units (AFU).

a-c, Mean biostain levels detected in *Varroa* after 24 hours of exposure to stained host bees (**a**). Levels of the fat biostain (Nile Red) are higher than that of the hemolymph (Uranine) biostain and appear in the same proportion as in the fat body of the host bees (**b**), Proportion Test (*prop test*): ($\chi^2=3.62e-28$, $P=1$). This proportion differs significantly from that of the hemolymph of these bees (**c**) providing further evidence that mites are not consuming this tissue in significant amounts (*prop test*: $\chi^2=197.33$, $P<0.001$).

Figure 3

32

Figure 3 Mites fed honey bee fat body tissue survived longer and produced more eggs than mites provisioned hemolymph. High mortality was observed across treatments; likely owing to the artificial setting. After 3 days, mites receiving 0%:100% and 25%:75% hemolymph:fat body as their diet maintained survivorship at 60% while the 100%:0% hemolymph:fat body and the starvation control had already exhibited full mortality.

a,b, Survivorship curve showing starvation control and all five host tissue diets (**a**). **b**, represents the same data with levels combined that show no difference in survivorship. Note, mites provisioned hemolymph and mites given no food showed no difference in survivorship. However, survivorship differed substantially between the hemolymph treatment and all treatments given any level of fat body ($\chi^2= 16.1$, $P<0.001$).

c, Average survivorship of mites differed by diet. Survivorship and the ratio of fat body by volume adhere to a strong positive linear relationship ($R^2=0.9634$).

d, Egg production differed between treatment diets (ANOVA: $P<.004$). A positive linear relationship was observed between egg production and the amount of fat body in the diet of the mite ($R^2=0.7894$).

Figure 4.1

42

Figure 4.1 SDS reducing gel and associated western blot comparing proteins present in mite and honey bee tissues. Lane 1 is blank, followed by a pooled sample of hemolymph and fat body from white-eyed drone pupae, hemolymph and fat body from white-eyed worker pupae, homogenate of honey bee eggs, blank, homogenate of *Varroa* mite eggs, full body homogenate of gravid *Varroa* mites, blank, and a molecular weight marker.

a, SDS reducing gel showing several proteins present in different honey bee and *Varroa* mite tissues. Note the well-defined, conserved bands of the molecular weight corresponding to honey bee vitellogenin and a cleaved fragment found only in honey bee fat body tissue.

b, Western blot identifying vitellogenin at two distinct molecular weights using a custom polyclonal antibody. These bands correspond to the full-length fragment of vitellogenin just below 200 kDa and the N-terminus fragment just above 40 kDa. As is to be expected the honey bee egg produced the most intense immunological response to the antibody with vitellogenin and the biochemically similar vitellin being the primary constituents of early stage eggs.

Figure 4.2

43

Figure 4.2 Details of *Varroa* reproduction studied via LT-SEM. Late stage gravid *Varroa* produce an egg comprising a substantial portion of their body volume every 30 hours representing an accelerated reproductive capacity. The volume of the developing oocyte is so large that it results in conspicuous differences in appearance between late and early stage gravid females.

a, b, showing fine details of a *Varroa* egg at 200x (**a**) and a size comparison between an egg and a gravid female 40x (**b**). The egg is oviposited by the female with an already well-developed protonymph inside. Note the distinctive imprint of legs and palps visible through the thin chorion.

c,d, Oviposition is imminent for the female imaged in panel (**c**); a state characterized by a generally bloated appearance and taut interscutellar membrane most conspicuously visible posterior to the anal plate. Compare with panel (**d**) in which the female shows appearance characteristic of early stage or suspended oocyte development.

Figure 5.1

53

Figure 5.1 LT-SEM comparison of two distinct morphotypes and three observed sizes of *Varroa destructor* collected from the same honey bee colony.

a, b, showing typical (**a**), atypical (**c**), intermediate form of *Varroa destructor*. The atypical specimen was substantially smaller than even the smallest recorded specimens of *Varroa jacobsoni*. In addition, it possessed a pentagonally shaped anal plate rather than the typical triangular appearance and a distinct, strongly spiculated cribrum. The intermediate specimen

was within the size range of *Varroa jacobsoni* (**b**). All specimens were identified as *Varroa destructor* based on genetic analysis.

Figure 5.2

55

Figure 5.2 LT-SEM observation of the setae arising from the dorsal shield of *Varroa destructor*.

a-f showing pilose setae of the dorsum of *Varroa* (**a**) and the venter of a honey bee (**b**). Morphological similarity between them may be an adaptation to establish tactile camouflage to avoid host grooming. *Varroa* feed beneath the ventral sclerites of the honey bee with a portion of their body exposed (**c**). Hairs point away from the body of the mite in the same direction as from the body of the host (**c, d**). Grooved, spine-like setae can also be seen on the edge of the dorsal shield (**a, e, f**).

Figure 5.3

56

Figure 5.3 LT-SEM observation of the fine structure and shape of the dorsal shield of *Varroa destructor*.

a,b showing the reticulation present across the entire surface area of the dorsal shield (**a**). The plates composing the dorsum and venter of the honey bee show very similar reticulation (**b**), likely further adaptation toward tactile camouflage.

c,d showing distinctive glabrous region comprising the anterior margin of the dorsal shield. Reticulation can be observed without being obscured by setae as is the case for the rest of the dorsum.

e,f the domed shape of the dorsal shield allows the parasitic mite to create and passively maintain a feeding chamber on the host bee.

Figure 5.4

60

Figure 5.4 LT-SEM observation of the fine structure of the ventral sclerites of *Varroa destructor*.

a, legs were removed from a mite to image the exopodal sclerite which sits behind the coxae of the bee. This plate merges with the plates of the peritremes on each side of the mites body. White arrows denote the regions where the exopodal sclerites becomes indistinguishable from the peritrematal shields.

b-e showing the plates that comprise the venter of a *Varroa* female (**b**). Note the variable chaetotaxy on the horseshoe shaped dorsal shield along the margin of the coxae (**b,c,e**). The arthroal membrane normally hidden by the sternal shield is visible sometimes in gravid mites (white arrow).

f showing comparison of setae on the dorsum with those on the venter. Pilose setae, similar in structure to those of the host, are only present on the dorsum. Simple setae, dissimilar from those present on most of the host are hidden on the underside of the mite.

Figure 5.5

61

Figure 5.5 LT-SEM observations detailing variability in the anal sclerite of *Varroa destructor*.

a-d showing the typical shape of the anal plate (**a**) which forms a triangle with the anus at the lower point of the triangle. Note the one seta arising near the anterior margin of the sclerite (white arrow). The presence of this seta was atypical in our specimens. Image (**b**) details an atypical pentagonally shaped anal sclerite observed in a markedly small individual. Note the differences in shape and spicule definition on the normally crescent shaped cribrum (**a-d**). The specimen in image (**b**) was the only specimen collected with such a distinctive cribrum.

Figure 5.6

64

Figure 5.6 LT-SEM observations detailing the structuring of the gnathosoma of *Varroa destructor*.

a, gnathosoma was separated from the body of the host dissected to show the complex constitution of this feeding structure. The chelicera arise dorsally with respect to the subcapitulum and corniculus. Well-developed salivary stylets (white arrows) arise on either side of the pre-oral trough and rest along the inner faces of the corniculus for much of their length. The fixed digit of the chelicera, normally similar in size to the mobile digit, has been reduced considerably and moved to a lateral position on the inner face of the mobile digit (brown arrow). A dorsal lyrifissure rests immediately proximal to the mobile digit on the middle article of the chelicera (black arrow).

b-d showing the cheliceral keel present on the inner face of each mobile digit (**b**) (white arrow). The keel on both chelicera can be pushed together to form a ridge (**d**, brown arrow) which seals and forms the roof for the tube-like feeding structure. The teeth along the top of each mobile digit are visible from bottom (**c**) of the chelicera as a result of the angling caused by the cheliceral keels as they are pushed together.

e, corniculi separated from the rest of the gnathosoma. Note the 6 denticles on the ventral edge on both corniculi. This feature varied periodically in specimens between 5 and 7.

f, showing the feeding wound inflicted by *Varroa* on adult an honey bee. Note that the shape of the chelicera when held together as one unit fits with the shape, size and general architecture of the wound.

Figure 5.7

66

Figure 5.7 LT-SEM observations detailing variable structuring of the subcapitular groove, tritosternum and palps of *Varroa destructor*.

a, showing the subcapitular groove with fine, irregularly spaced clusters of denticles populating the inner surface (black arrow). Irregularly spaced rows of denticles also arise from the dorsal surface of the tritosternum likely fitting together with those in the groove forming a process that sieves out any stray particulate matter that may be present in the host meal.

b, c, showing the tritosternum housed in the subcapitular groove (**b, c**). Varying numbers of micropili of unknown (possibly sensory) function arise from the ventral surface of the gnathosoma (black arrows). Between 7 and 14 micropili were present in specimens collected for this study. Note some denticles of the dorsal surface of the tritosternum are visible as well (white arrows).

d, e, the last segment (apotele) of the palp bears a variable character of a small tooth between the large and small claw (**d**, white arrow) in some specimens. Most specimens lacked this trait with a totally smooth region present between the long and short claw (**e**, black arrow).

f, showing the indentation of the palps and gnathosoma of a mite in the intersegmental membrane of an adult host bee. Note the position of the indentation caused by the apotele (white arrow). Only the indentation of the long claw is present. Based on the orientation of the claw pressed against the host membrane the short claw is likely embedded in the membrane to potentially gain leverage to facilitate the gnathosoma piercing the membrane. The long claw appears to be used as a brace against the tissue.

Figure 5.8

70

Figure 5.8 LT-SEM observations detailing the structure of and characters associated with legs of *Varroa destructor*.

a, showing the legs of *Varroa* which are separated into sensory (leg I) and ambulatory (leg II, III, IV).

b, reticulation clearly visible on the lateral faces of coxae (white arrow) but becomes faint to indistinguishable on the dorsal and ventral surfaces.

c, foundress mite with wounds typical of “ankle biting” genetic line of honey bees. Note, the missing ambulacra from legs I (white arrow). Surprisingly, this mite was still able to find and reproduce normally within a brood cell even with a portion of its primary sensory structure missing.

d-f, showing a fine process of denticles following the distal margin of the coxa of leg I (white arrows). These denticles arise along the lateral edges of the margin and to some extent are present in the region of the coxae behind leg I (**e**).

Figure 5.9

71

Figure 5.9 LT-SEM observations detailing the structure of and characters associated with the ambulacra of *Varroa destructor*.

a, showing an ambulacrum of *Varroa* on an ambulatory leg in its “foot-down” conformation. The shape of the ambulacrum changes noticeably when free or attached to a surface. On each ambulatory leg, a pair of small, likely sensory, setae are present in indentations on either side of the ambulacrum (white arrow). These setae likely function proprioceptively informing the mite of the position of its ambulacrum.

b, ambulacra of ambulatory legs (II and III). Note setae at the base of the ambulacra (black arrows).

c,d, the difference between the free (**c**) and attached (**d**) conformation of the ambulacra on the sensory pair of (leg I) is more pronounced than the difference in the ambulacra of the ambulatory legs. Note the setae on the lateral section of the ambulacrum is not present in the sensory legs.

e,f, showing the ambulacra when attached to an adult honey bee host. The mite is wedged in a pocket of tissue between segments of the bee. The ambulacra of leg I holds especially well to the membrane in this region (**f**). When the mite is removed in a while frozen

Figure 5.10 LT-SEM observations detailing the structure and variability in characters associated with the peritreme and stigma of *Varroa destructor*.

a,b,c showing variation in the terminal point of the peritreme. The peritreme appears to terminate in a slit that runs perpendicular to the path of the rest peritreme (**a,b** white arrows). In most specimens the peritreme terminates in this region and does not connect to the stigma (black arrows). Alternately, in some specimens the peritreme crosses this perpendicular slit and terminates at the stigma (**c**). Note the rugulose intersegmental membrane surrounding the peritreme (**a,b**).

d,e. showing the peritreme when at its resting conformation. This unique pseudo-appendage conforms to the shape of the dorsal shield and leg of the mite.

f, showing raised peritremes apparently characteristic of mites facing respiratory challenge (white arrow). Moving the peritremes can allow the mite to avoid suffocation when submerged in fluid.

General Introduction

The honey bee genus *Apis* is far from the most speciose of the bee genera (composed of just 10 of the 20,000 bee species (1), but it is certainly the most profitable and well known. The economic value attributed to their pollination services alone totals nearly \$12 billion annually in the US (2). Global food security is similarly dependent on honey bee pollination with 65% of 107 leading global crop commodities requiring or being amplified substantially by *Apis* pollination (3). Recent declines in honey bee health and concomitant colony losses have spurred greater research interest in honey bees and the stress factors impacting their populations globally. These studies have widely concluded that the documented decline in honey bee health is driven by a confluence of factors both biotic and abiotic (4) but the most significant driver is the mesostigmatid parasite *Varroa destructor* (5, 6).

Potentially owing to honey bee diversity unrivaled by other regions and a long shared history, Asia has the greatest diversity of honey bee parasitic mites. With the exception of *Acarapis woodi*, the parasitic mites now exploiting *A. mellifera* were exclusively parasites of Asian honey bees. *V. destructor* (henceforth, *Varroa*) originally parasitized *Apis cerana*, the Eastern (or Asiatic honey bee) honey bee (7). Long evolutionary history in sympatry has allowed for *Varroa* to have a balanced host-parasite relationship with its original host. The Eastern honey bee has a number of effective defenses to maintain the parasite at asymptomatic levels (8, 9). However, phylogenetic evidence suggests that its relationship with the Western (or European) honey bee, *A. mellifera*, began far more recently (between 50 and 100 years ago) and as such very few, if any, of these defenses exist in the European honey bee (5, 10).

Varroa began spreading across the globe about 5 decades ago and has since achieved a nearly cosmopolitan distribution. It is currently found in virtually every *A. mellifera* colony around the world excluding Australia and small outlying island territories (5). This invasive mite was first detected in the US in 1987 (11). Within a decade of its introduction, *Varroa* had wiped out nearly all established feral honey bee colonies (11). Managed colonies have experienced heightened losses as well though not at the magnitude of the feral colonies due primarily to the intervention of beekeepers. The cost of managing *Varroa* factors substantially into the conservative \$120 billion estimate of the economic damages of invasive species in the US each year and the \$1.41 trillion worldwide which represents 5% of the global economy (12, 13). Developing countries are more dramatically impacted by invasions like that of *Varroa* because of their greater reliance on agriculture (13).

Without intervention, most colonies will die within 1 to 2 years of infection (14). Just 5 decades ago, colonies were observed collapsing 4-5 years post introduction of *Varroa* into the colony. Honey bees reportedly could tolerate mite loads of several thousand mites per 10,000 bees before reaching critical threshold(15, 16). Now a ratio of 3% brings the colony to its critical threshold suggesting that mite populations are growing in virulence or that the bees are becoming less tolerant (17). The reasons for this potential growth in virulence are poorly understood but may relate to the introduction and/or hybridization of different *Varroa* haplotypes which have been shown to vary in virulence (7, 11). Studies in Asia have shown hybridization between the 9 *V. destructor* haplotypes producing hybrids of undetermined virulence and host range (9).

The need for consistent chemical intervention and increased losses have driven up the cost of beekeeping, ostensibly pricing the practice out of reach of many lower income, would-be beekeepers. Further, in the years since its introduction, our agricultural dependency on pollinator-dependent crops has increased considerably underscoring our need to better understand this parasite and develop more effective control measures (18). However much of our understanding of the fundamentals of this parasite's morphology, behavior and lifecycle is based on studies published in the former Soviet Union most of which have never been translated into English. As a direct result, many conclusions about this species have been drawn from studies for which methods have not been reproduced and claims never verified.

Chapter 1: Determining the Feeding Site of *Varroa destructor* on Adult Honey Bees: Is There Actually a Phoretic Phase?

Introduction

Varroa destructor (*Varroa*) is the most significant single driver of managed European honey bee (*Apis mellifera*) colony losses worldwide (5). Several factors contribute to the dramatic effect of *Varroa* on honey bee populations including the direct impact of their feeding on immature bees, their status as a confirmed vector of five debilitating viruses and potentially 13 others, their near ubiquitous presence in *A. mellifera* colonies, and the naïve nature of the host and parasite to one another due to

their lack of historical sympatry (5, 19, 20). All of these factors have been studied extensively over the last half century but the conclusion that *Varroa* feed exclusively on the hemolymph of honey bees (hemolymphagy) has received little discernible scrutiny. Notably, multiple studies have been undertaken to explain the diverse array of honey bee pathologies associated with *Varroa* feeding that cannot be attributed to the removal of a small volume of hemolymph (21-28). These pathologies range from diminished immune function and reduced pesticide tolerance to impaired pupal development and shortened lifespan underscoring an imperative to understand exactly how parasitic feeding impacts an insect critical to global food security (5, 22, 24, 25, 27).

While vertebrate blood-feeding (hemophagy) is well-documented in arthropods, the substantially lower nutrient content of insect hemolymph calls into question the ability of an organism to sustain itself exclusively on this resource (29-31). Vertebrate blood has a cell content of about 40% by volume contributing to a relatively high nutrient content. Insect hemolymph generally contains less than 2% cell content and has a generally dilute nutrient profile (32, 33). In line with these facts, the concept of hemolymph feeding as the sole or main nutrient acquisition strategy has been addressed and largely refuted in several insects (29-31, 34-37).

Our current understanding of *Varroa* feeding behavior is based on work conducted in the 1970s in which investigators used radioisotopes, [⁹⁰Sr] or [³H], to conclude that the mites feed on their host's hemolymph (38-40). [³H] lacks consistency as a marker for target tissue and has since fallen out of favor (39, 40). [⁹⁰Sr] was used as a marker for hemolymph because of its tendency to replace calcium in tissue but the

abundance of calcium in both hemolymph and fat body makes it impossible to identify a host meal in the presence of both tissues via this method. The issues with using either isotope for this purpose would be further exacerbated if *Varroa* employs extra-oral digestion like most mesostigmatids, since liquid and semi-solid tissues would dissolve together in the host before consumption. Attempts to develop systemic chemotherapeutics during the same period (miticides fed to the bees and consumed by the mites when they feed) consistently ended in failure and as such, none are currently commercially available (5, 16). This is expected if the target host tissue has not been accurately identified. However, despite the failings of the experimental evidence and the existence of circumstantial evidence suggesting that this parasite feeds on a different host tissue, *Varroa* hemolymphagy has remained the accepted view.

Varroa are closely allied phylogenetically with predatory and parasitic mites that feed by extra-oral digestion (41). This implies that they may consume semi-solid tissue near where they attach to their host. Furthermore, the digestive system and mouthparts of this mite are structured in ways I would expect from an organism that feeds on semi-solid tissue via extra-oral digestion rather than hemolymph. For example, *Varroa* have simple, tube-like gut structuring, (no enzymatic activity in the midgut) and a gnathosoma with well-developed salivary stylets allowing salivary fluid to mix efficiently with internal host tissue (16, 42). While *Varroa* possess attributes associated with feeding on semi-solid tissue, they lack essential adaptations associated with hemolymph feeding. The evolutionary transition to dilute fluid feeding is usually accompanied by a reduction in sclerotization of the idiosoma which allows for the parasite to stretch to accommodate a large volume of liquid food (43). *Varroa* are

conspicuously lacking this adaptation along with characteristic restructuring of the digestive system (i.e., a filter chamber or analogous adaptation) to manage the added osmoregulatory burden of a low-nutrient, high water diet (16, 35, 44, 45). Further, the waste product excreted by this mite, i.e. guanine, is usually associated with organisms that have an abundance of protein in their diet and significant water limitation (46).

Considering the discrepancies between *Varroa* physiology and what I would expect from a hemolymphage, I have proposed an alternative hypothesis that *Varroa* feed on honey bee fat body tissue. Such a feeding behavior is more consistent with our current understanding of the morphology and physiology of *Varroa* and the diversity of pathologies associated with its feeding. Fat body is a nutrient rich, vital organ near the cuticle of both adult and immature honey bees (47). It is the primary site of protein and urate synthesis and contains relatively high levels of guanine (47, 48). The essential role of the fat body in hormone regulation, immune response, and especially pesticide detoxification makes an understanding of the relationship between this parasite and this tissue particularly relevant to ongoing discussions on the causes of honey bee health decline (47). Moreover, determination of the primary source of nutrition for *Varroa* would change our understanding of the etiology of this parasite and could potentially lead to the development of novel, and of active interest, more effective, treatment strategies (e.g. systemic pesticide formulations, RNAi, etc.). To that aim, I conducted a three-tiered study asking the following questions: 1) Do so-called phoretic *Varroa* primarily or exclusively feed in proximity to the fat body? 2) What host tissue(s) is (are) being ingested by *Varroa* when feeding? 3) What host tissue(s) is (are) integral to survivorship and reproduction in foundress mites?

Methods: Spatial Distribution of Apparently Feeding Mites on Adult Bees

To determine the location of dispersing mites on adult bees in *A. mellifera* colonies, I examined bees originating from naturally mite infested colonies maintained by the University of Maryland or United States Department of Agriculture, Agricultural Research Service (USDA ARS) Bee Research Lab in Prince Georges County, Maryland. Between May and June 2016, frames containing capped and uncapped brood were removed from 4 different colonies on 8 occasions. Sampling was conducted during favorable beekeeping weather (i.e. while sunny and warm) to permit opening hives with minimal usage of smoke, minimizing the potential impact on parasite behavior. Immediately after removal, worker bees were randomly selected, pulled from the frame by clasping the wings together and inspected for the presence of *Varroa*. The location of the mite was recorded being on the head, between the head and mesosoma, on the mesosoma, between the mesosoma and metasoma, or beneath an ordinal numbered tergite or sternite on the metasoma (24 locations total). Examined bees were removed from the colony to avoid sampling the same individual multiple times. Data from drones was not collected in this study.

Methods: Transmission Electron Microscopy & Light Microscopy

Adult bees were taken from *Varroa* infested colonies, and a single drop of cyanoacrylate glue was placed on actively feeding mites. The glue permanently affixed the position of the mite between the tergite and/or sternite of the bee. The head and thorax of the bee was removed and the abdomen with attached mite was fixed in 2.5% glutaraldehyde, 0.05M sodium cacodylate for 2 hours. After initial fixation, the abdomen was further dissected and trimmed to a size encompassing the area directly

around the mite, and a small cut was made in the posterior end of the mite to facilitate fixation and embedding. The bee/mite complex was fixed at 4°C overnight, then the tissue was rinsed 5 times with 0.05M cacodylate buffer and post-fixed in 1% buffered osmium tetroxide for 2 hours at room temperature. The tissue was then rinsed 5 times in the same buffer, dehydrated in a graded series of ethanol followed by 2 exchanges of propylene oxide, infiltrated in a graded series of LX-112 resin/propylene oxide and polymerized in LX-112 resin at 65°C for 24 hrs. 60-90nm silver-gold sections were cut on a Reichert/AO Ultracut ultramicrotome with a Diatome diamond knife and mounted onto formvar-coated copper slot grids. Grids were stained with 4% uranyl acetate and 3% lead citrate and imaged at 80kV with a Hitachi HT-7700 transmission electron microscope. For light microscopy, 0.5µm thick sections were mounted onto glass slides, stained with toluidine blue, and imaged with a *Zeiss Axiozoom VI6* stereo zoom microscope.

Methods: Low Temperature Scanning Electron Microscopy

Low temperature scanning electron microscopy was conducted at the USDA ARS Electron and Confocal Microscopy Unit using techniques outlined by Bolton et al. (2014) (49). *Varroa* parasitized honey bee metasoma were dissected to expose the feeding mite. Each metasoma was were secured to 15 cm x 30 cm copper plates using ultra smooth, round (12mm diameter), carbon adhesive tabs (Electron Microscopy Sciences, Inc., Hatfield, PA, USA). The specimens were frozen conductively, in a Styrofoam box, by placing the plates on the surface of a pre-cooled (-196 °C) brass bar, the lower half of which was submerged in liquid nitrogen (LN2). After 20-30 seconds, the holders containing the frozen samples were transferred to a Quorum PP2000 cryo-

prep chamber (Quorum Technologies, East Sussex, UK) attached to an S-4700 field emission scanning electron microscope (Hitachi High Technologies America, Inc., Dallas, TX, USA). The specimens were etched inside the cryo-transfer system to remove any surface contamination (condensed water vapor) by raising the temperature of the stage to -90 °C for 10-15 min. Following etching, the temperature inside the chamber was lowered below -130 °C, and the specimens were coated with a 10nm layer of platinum using a magnetron sputter head equipped with a platinum target. The specimens were transferred to a pre-cooled (-130 °C) cryostage in the SEM for observation. An accelerating voltage of 5kV was used to view the specimens. Images were captured using a 4pi Analysis System (Durham, NC).

Results

To answer the first question, I conducted an observational study wherein I mapped the location of *Varroa* parasitizing adult bees. I hypothesized that the mites would not randomly disperse on adult bees, but rather, would be found preferentially at sites on the bee that maximized their ability to access their target food source. Fat body is distributed throughout the hemocoel of immature bees but in adult honey bees it is primarily localized to the inner dorsal and ventral surfaces of the metasoma (the designation for the abdominal region in hymenoptera) (50). I examined worker bees in the brood nests of four different colonies, of which 104 had at least one mite present. I found clear location biases in these mites (Figure 1.1). The majority (n=99, 95.2%) were found ventrally on metasoma wedged underneath the overlapping terga or sterna (abdominal plates) of the bee (Figure 1.2a & b). Specifically, mites on the metasoma

were found with greatest frequency (88.5%) underneath the sternite or tergite of the third metasomal segment (Figure 1a). No mites were found on the head of the host bee. Few mites were found on the mesosoma (thoracic region) of the host (about 4.8%). Notably, these mites behaved differently than the mites beneath the sterna and terga; they moved about actively and were primarily found with their sensory legs raised suggesting that they were questing for transfer to a passing bee rather than feeding. Upon removal of the mite, I found no evidence of feeding in this location. Mites on the metasoma moved only after being disturbed repeatedly. *Varroa* located on the metasoma of the host also exhibited a consistent preference for the left side (74.8% of observations) (Figure 1.1 a).

The life cycle of *Varroa* is separated into two distinct phases that focus on separate life stages of the bee, the reproductive (parasitizing the brood) and the so-called “phoretic” (parasitizing adult bees). The term “phoretic” is defined by exploitation of a host for transport and specifically excludes exploitation of the host as a food source (51-58). To determine if these mites were truly phoretic (i.e. seeking only transport, harborage, and/or protection from grooming under the sternites and tergites of the host bee), I examined the intersegmental membrane in the area of highest preference. Images captured via low-temperature scanning electron microscopy revealed a wound in the intersegmental membrane (Figure 1.2c & d) caused by the gnathosoma of the mite (Figure 1.2e). Freeze-fractures of bees with attached mites show that these parasites feed in close proximity to fat body and soft muscle tissue (Figure 1.2f). To better image the wound site, adult bees with apparently feeding mites were chemically fixed, thin sectioned, and imaged via transmission electron

microscopy. In addition, several 0.5 μ m thick sections were slide mounted, stained, and imaged with via light microscopy. These methods show a mound of host tissue at the wound site (Figure 1.3a-c). Just below the surface of the wound are the inner contents of damaged fat body cells showing degradation consistent with extra-oral digestion (Figure 1.3c & e). Further, these images also reveal two colonies of morphologically distinct bacteria (Figure 1.3c & d) similar to observations of bacteria colonizing *Varroa* feeding wounds in brood (59).

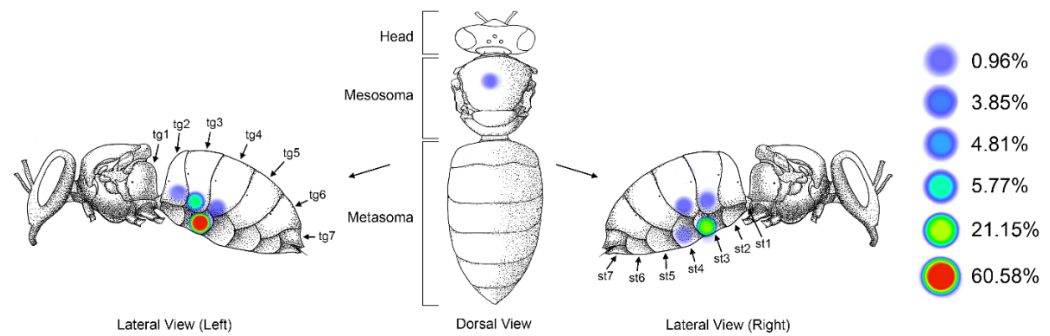


Figure 1.1

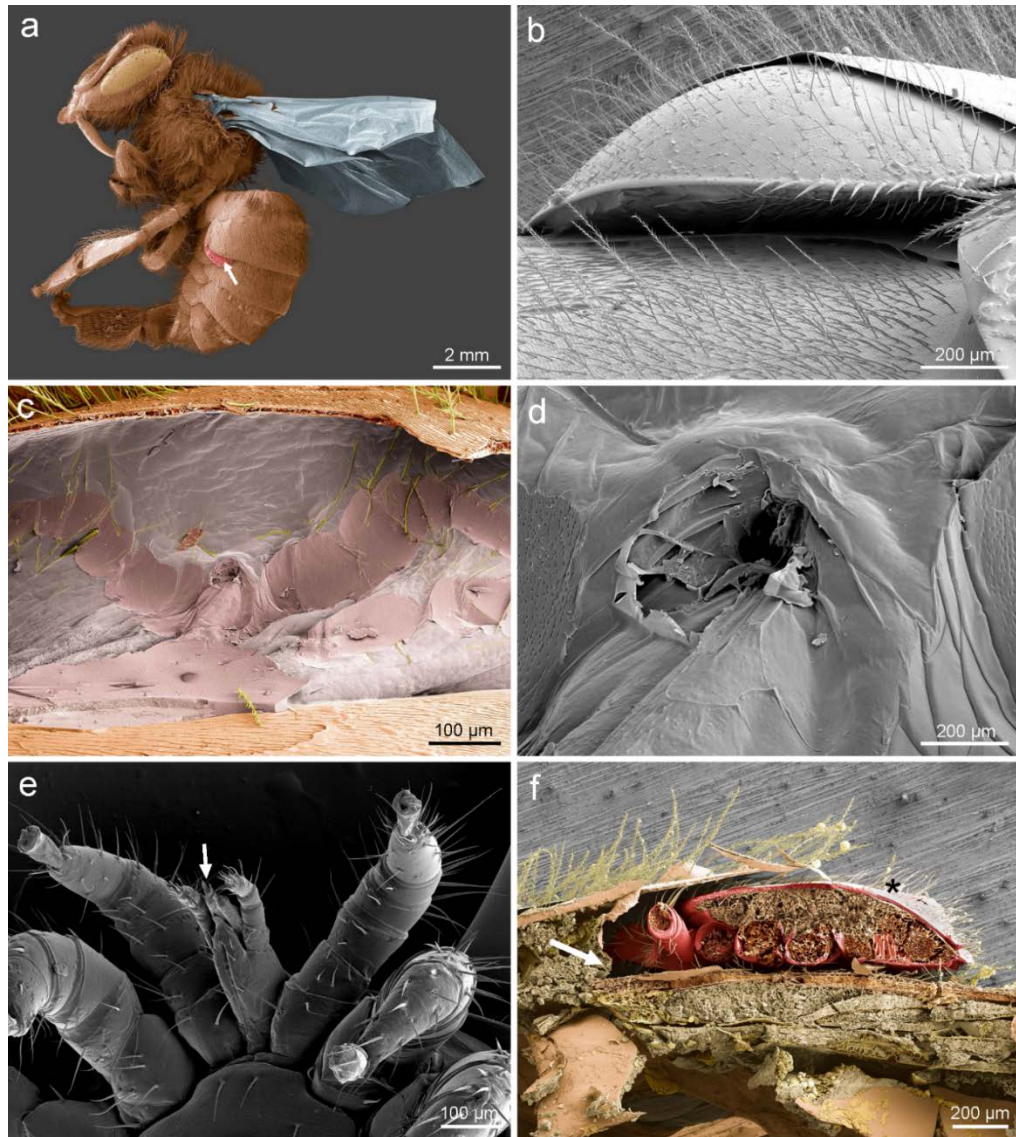


Figure 1.2

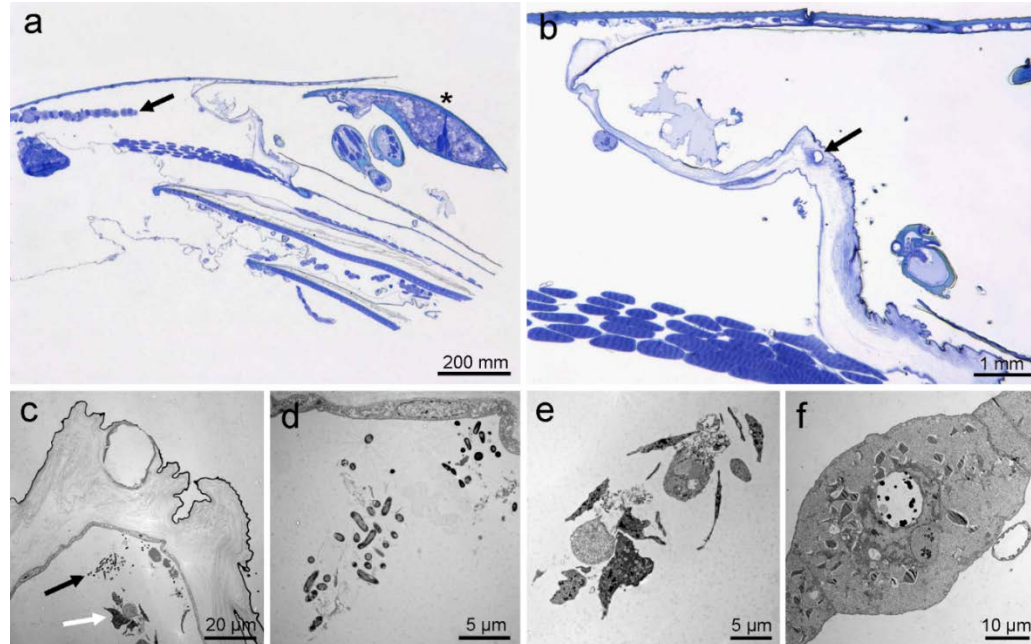


Figure 1.3

Figure 1.1 *Varroa destructor* shows consistent preference for the underside of the metasoma of adult host bees, an area predominated by fat body tissue just beneath the cuticle.

a, Diagram showing frequency of dispersing *Varroa* found in each location on 104 parasitized worker bees in five trials (tg=tergite, st=sternite). *Varroa* were found on the underside of metasoma as opposed to locations on the mesosoma or head (GLM: $\chi^2 = 6.5$, $P < 0.001$). Mites strongly preferred the third segment of the metasoma to any of the other 23 locations (GLM: $\chi^2 = 4.5$, $P < 0.001$). Mites were also found preferentially on the left side of the host (Chi: $\chi^2 = 24.02$, $P < 0.001$).

Figure 1.2 Feeding site of *Varroa* in dispersal phase imaged on adult honey bee via Low Temperature Scanning Electron Microscopy (LT-SEM).

a-e, Colorized image of a worker bee parasitized by *Varroa* (white arrow) (**a** & **b**). The mite is wedged beneath the third tergite of the metasoma. When removed, a wound can be observed (**c**, **d**) matching the modified chelicera of the mite mouthparts (**e**). Image **c** colorized to show the impression of the mite left in the soft tissue of the bee.

f, Freeze fracture image showing a cross section of a mite at feeding site; note the thin intersegmental membrane (white arrow) and fat body and muscle tissue just on the other side. In the process of creating the fracture, the mite (black asterisk) was pushed away from the membrane.

Figure 1.3 Dispersing *Varroa* attached to worker bees were used to pinpoint the precise location of the feeding site, revealing the ultrastructural morphology of the feeding site wound, bacteria at the feeding site, and details of the fat body.

a,b, Histological cross section of a worker bee with *Varroa* attached in the feeding position at the third metasomal segment, arrows showing position of the fat body tissue lying directly beneath the intersegmental membrane (**a**). The feeding site wound in the

membrane of the bee is clearly visible as a large mound with a hole intersecting the membrane, arrow indicating the hole (**b**).

c-e Transmission electron microscopy (TEM) images of the feeding site wound in the intersegmental membrane of the bee, showing a hole with irregular edges where the chelicera of the mite have penetrated the membrane. The black arrow indicates bacteria at the feeding site beneath the intersegmental membrane, and the white arrow indicates degraded fat body cells likely due to the extra-oral digestion. (**c**) Higher magnification reveals two species of morphologically distinct bacteria (**d**) and greater detail of irregularly shaped cell contents of the degraded fat body tissue (**e**).

f, TEM image of the fat body tissue showing a trophocyte with numerous vacuoles filled with electron dense lipid globules and an irregularly shaped nucleus.

Discussion

These images constitute direct evidence that *Varroa* feed on adult worker bees and are not using them for phoresy. Exceptions have been made historically for some parasites such as *Macrocheles muscaedomesticae* which may or may not feed briefly while in transit because transport to a specific destination is the primary goal, feeding is not consistent, and the parasite is not specialized for the task (53, 60, 61). This exception, however, cannot be made for *Varroa* as these mites utilize adult host bees for feeding consistently, their shape and anatomy is adapted for fitting between the plates of these bees to access their feeding site, and they remain in this phase for several days showing that transport from one specific location to another is not the primary goal (62, 63). *Varroa* remain attached to adult bees between 1 and 13 days with an average of about 7 days (63, 64). If the primary goal of the mites is to be moved to a new reproductive host, the length of time spent on the adult host is unnecessary under most circumstances. *Varroa* are primarily found on nurse bees during this stage, and their frequent contact with viable brood would allow them to parasitize new brood

almost immediately. These observations are, however, consistent with behaviors expected from a parasite with the goal of obtaining essential nutrients from a host.

I would propose replacing the inaccurate term “phoretic phase” with the more accurate designation “dispersal phase”. Because feeding occurs consistently in both phases of the lifecycle of the mite, it is not useful to attempt to define either stage by the presence or absence of feeding. Instead, there is greater utility in defining the so-called “phoretic phase” by the most distinctive feature; mites can disperse to new brood cells (to juvenile hosts), between worker bees (adult hosts), and to new host colonies only in this phase (barring human intervention). The term “dispersal phase” will be used throughout to refer to so-called “phoretic mites”.

The preference for feeding on the ventral rather than the dorsal region of the metasoma is consistent with expectations if fat body is the target tissue as there are larger deposits of fat body tissue on the inner ventral surface of the metasoma rather than the dorsal surface (50). Preference for the third segment may be because it is the longest segment, providing a large external parasite with space to feed while concealing most of its body from a grooming host (Figures 1.1 & 1.2a). This theory is further bolstered by the observation that the mites consistently fed under the longest section of the longest segment, a lobe formed by the edge of each tergite or sternite (Figure 1.2b). The strong preference of this parasite for the left side of its host suggests that there may be a benefit to feeding in this location as well. This preference may be related in part to asymmetry in host grooming habits or internal asymmetry of the host. Our dissections have shown that a larger section of the ventriculus (gut) rests on the left side of the honey stomach and rectum than the right side. Full expansion of the honey

stomach or rectum (a common occurrence during feeding or digestion) would theoretically push this section farther to the left forcing it against the body wall on the left side. This likely forces the fat body tissue closer to the cuticle potentially making more of it accessible to the parasite.

Chapter 2: Identification of Host Tissue Consumed by Parasitic Mite *Varroa destructor* Using Tissue Specific Fluorescent Biostains

Introduction

While our observational and histological work provide evidence for fat body feeding, I confirmed these findings by differentially staining both target tissues in host worker bees and examining the contents of the mites that were allowed to feed on these bees. Bees were fed a fluorescent lipophilic biostain, Nile Red, to mark the fat body tissue and a fluorescent hydrophilic biostain, Uranine, to mark the hemolymph. Both biostains were confirmed to persist in their target tissue (Figure 2.1 **a-d**). Samples of bee hemolymph, fat body, and gut were removed from the biostained host and imaged using fluorescence microscopy. Fluorescence from the digestive system of the mite was captured directly through the integument of the mite (Figure 2.2 **a & b**). Mites fed a diet with a single biostain were imaged via confocal laser scanning microscopy. I removed the genital and posterior metapodal plates from these mites to better resolve internal structures (Figure 2.2 **c-e**).

Methods: Tissue Biostain Study

Frames of capped brood were collected from treated colonies maintained by the University of Maryland, College Park. Each individual frame of capped brood was placed in a ventilated, single frame box (custom designed by Zastrow Services LLC)

and placed an incubator at 34°C and 80% RH. Emerging adult bees were collected at least once every 24 hours.

Varroa used in this experiment were obtained from untreated colonies. These colonies were maintained by the University of Maryland, College Park or the USDA ARS and were sampled between June and late August. Adult honey bees with apparently feeding *Varroa* (located at the identified feeding site) were collected and the mites allowed to remain on the host bees until they were needed later in the study.

Adult honey bees were confined to cages with approximately 30 individuals of the same age. Cages consisted of 16oz transparent *Solo* brand cups with nylon mosquito netting used as a lid to maintain adequate ventilation. Feeders were made from 2ml microcentrifuge tubes. A hole was made in the bottom of each feeder with a heated metal probe. Four feeders were suspended through small holes cut in the mesh lid of each cage.

Fluorescent biostains were used to stain the relevant tissues. Uranine (*ThermoFisher*), was selected to mark the hemolymph because of its low lipophilicity (k_{ow} : 0.0342) and high water solubility (500,000 mg/L). Nile Red (*ThermoFisher*) has the inverse of these characteristics (k_{ow} : 4.38, solubility: 0.178 mg/L) and as such was used as the fluorophore to mark the fat body.

The diet consisted of 30g of sucrose dissolved in 100ml of distilled water. A 2% mixture of Uranine was made from 2g of sodium fluorescein powder dissolved in 98ml of distilled water. Then 1.5ml of the 2% Uranine mixture was added to the sugar water diet. A mixture of 0.025g of Nile Red biostain powder dissolved in 0.5ml of sunflower oil was added to the solution. Soy lecithin (0.5g) was added to act as an

emulsifier and 5g of honey as a stabilizer for the emulsion. The entire mixture was blended for 1 minute in a high speed *Nutribullet* blender (*Pro 900 Model*) to ensure thorough mixing of the emulsion. Honey bees were allowed to feed on this solution *ad libitum* immediately post eclosion for 5 days.

I also introduced *Megabee* pollen substitute as a source of protein. Burr comb was removed from several honey bee colonies and placed into the aforementioned rearing cages. I created a 100ml, 1:1 mixture of pollen substitute to heavy sugar syrup (composed of 2:1 sugar to distilled water). I then added 5ml of sunflower oil mixed with 0.025g of Nile Red powder and 1.5ml of the 2% Uranine mixture. This pollen/fluorophore mix was added to about 20 cells per comb.

At 5 days post eclosion, biostain-fed bees were removed from the colony cups and each placed in a small transparent 1.25oz *Solo* cup with nylon mosquito netting used as a lid to ensure that the mites were not able to escape. A single dispersal phase *Varroa* female was placed on the body of each adult bee. The bee was allowed to feed on a 30% sugar solution *ad libitum* from a partially filled 2ml microcentrifuge tube suspended through a hole in the mesh lid. This sugar solution lacked biostain to prevent mites from picking up biostain from the feeder or potential spills while confined with the experimental host bee. Bees in our cage studies showed far greater survivorship when confined with burr comb so small sections of burr comb (9 cells) were cut out and placed in these small cups as well. Pollen mix without either biostain was added to 4 cells.

After the trial, the *Varroa* were removed from their host bees. The mites were then rinsed with 70% ethanol to remove biostain that may have potentially contacted

the mite's integument from the excrement or regurgitation of the host. The experimental mites were then placed in fluid exchange vessels, 1 mite per numbered well to allow for continued association of the mite with its specific host bee. These fluid exchange vessels were then submerged in 30% peroxide for 5 days to quench the autofluorescence of the integument of the mite. After the peroxide bath, fluorescence levels of the internal structures were acquired and quantified using a *Zeiss Axiozoom V16* stereo zoom microscope. Images of the mites were captured at 40x magnification at 1s exposure. Fluorescence values were aggregated using ImageJ software and analyzed with R statistical computing software version 3.4.2.

Tissue was extracted from each experimental bee to verify that the correct biostain accumulated in the target tissue. Using a *Finnpipette* brand 10 μ l micropipette, 2 μ l of hemolymph were withdrawn from each bee. Afterwards, the gut contents were removed from the bee by carefully pulling out the digestive tract via the stinger. If the digestive tract showed any signs of tearing, that sample was discarded to avoid gut contents spilling onto the fat body and causing inaccurate readings. Fat body was collected via dissection and about 2 μ l was measured using a *Finnpipette* brand 10 μ l micropipette. Fluorescence of honey bee samples was acquired using the same methods as those for *Varroa*. Samples were also collected via the same methods from honey bees fed sugar solution lacking any fluorophore. The mites fed on control bees submerged in 30% hydrogen peroxide and imaged to establish baseline autofluorescence levels for photochemically quenched mites. Tissue from the control bees was used to estimate average levels of autofluorescence naturally associated with

each tissue. The averages of these values were calculated and removed from those of the experimental mites prior to statistical analysis.

Our preliminary observations showed that *Varroa* rarely survived for 24 hours without feeding which corresponds with the findings of Garedew et al. (2004)(65). To reduce the likelihood that data from *Varroa* that had not fed on the biostain marked host were being included in this study, *Varroa* that died during the 24-hour trial were not processed or included in the data set. Trials in which the honey bee did not survive were also not included. Though *Varroa* have been shown to continue feeding from bees several hours after they die(65), hemolymph samples could not be obtained from dead bees so their data was also not included in the analysis.

Preliminary trials were conducted to establish the stability of each biostain in the target and non-target tissue. Adult bees were randomly assigned to one of two treatments, each fed only one of the biostains from the first day of emergence onward. After 5 days the levels of the biostain in hemolymph and fat body were collected and compared using the aforementioned protocols. Peroxide protocols were refined to ensure this chemical was not damaging the fluorophore. Mites fed biostain were submerged in peroxide for between 1 & 12 days to determine when autofluorescence was adequately quenched but the fluorophores were still active. This period was determined to be between 4 and 6 days.

Methods: Tissue Axiozoom Fluorescent Microscopy

A Zeiss AxioZoom V16 stereo zoom microscope (Thornwood, NY) was used to obtain images. The images were observed using a 1x 0.25NA or 2.3X 0.25NA

PlanNeoFluor objective. LED lighting was used for brightfield imaging and an AxioCam HRC Color camera was used to capture the images. Fluorescence microscopy was accomplished using a 200 watt mercury vapor lamp (HXP Short Arc Lamp, Thornwood, NY) with a filter set for YFP with excitation at 500nm, beam splitter 515nm and emission at 535nm; mRFP with excitation at 572nm, beam splitter 590nm and emission at 600nm. Fluorescence was captured using an AxioCam 506 mono camera. Zen 2 Pro Blue (Thornwood, NY) 64 bit software was used to capture and preprocess images.

Methods: Confocal Laser Scanning Microscopy

A Zeiss LSM710 confocal laser scanning microscopy (CLSM) system was utilized. The samples were mounted on slides and observed using a Zeiss Axio Observer™ (Thornwood, NY) inverted microscope with 10x 0.5 NA and 40x 1.2 NA Plan-Apochromat objectives. Several excitation wavelengths were utilized, 405nm (DAPI), 488nm (GFP), 515 (YFP) and 561nm (DsRed) with corresponding filter sets for each emission, 410-484nm (DAPI), 494-554nm (GFP), 530-555 (YFP) and 566-704nm (DsRed) with a pin hole of 33µm. Zeiss Zen 2012 Pro software was used to obtain 20-50 z-stack images to produce maximum intensity projections.

Results

Mites fed a diet with a single biostain were imaged via confocal laser scanning microscopy. I removed the genital and posterior metapodal plates from these mites to better resolve internal structures (Figure 2.2 **c-e**). Fluorescence associated with honey

bee fat body tissue was consistently detected inside of the mites comprising two to four times what was detected from honey bee hemolymph in the same mites (Figure 2.3 a-c). No mites from this study showed greater levels of the hemolymph biostain than the fat body biostain. The confocal images confirmed these findings as mites fed on bees with only biostained hemolymph (Figure 2.2d) showed fluorescence levels similar to the control (given no biostain) (Figure 2.2e). However, mites fed on host bees with fluorescently stained fat body tissue produced a robust signal of sufficient intensity to clearly see the shape of the digestive system of the mite (Figure 2.2c).

The distinct biochemical properties of each tissue allowed for a tissue-specific fluorescence profile to be determined. Fat body tissue has small amounts of hemolymph that run throughout. Hemolymph tissue contains low levels of lipophorin and circulating adipocytes so both tissues were expected to accumulate low levels of the non-target biostain. The proportion of fluorescence from the non-target biostain relative to the target biostain was used to create the unique profile for each tissue. Nile Red fluorescence over total sample fluorescence in honey bee fat body tissue yielded a value of 71.1% and 17.3% in the hemolymph (Figure 2.3b & c). Nile Red fluorescence relative to total sample fluorescence generated from mites exposed to biostained bees yielded a value of 71.6% (Figure 2.3a). There was no statistically significant difference between fat body fluorescence profile and the fluorescence profile of the mites after feeding on biostained bees, strongly suggesting that the tissue in the experimental mites is fat body tissue. However, the fluorescence profile of the hemolymph (17.3%) differed substantially from what was found in the experimental mites.

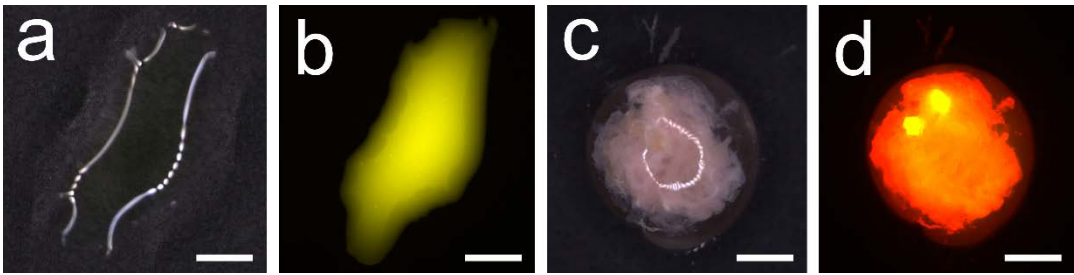


Figure 2.1

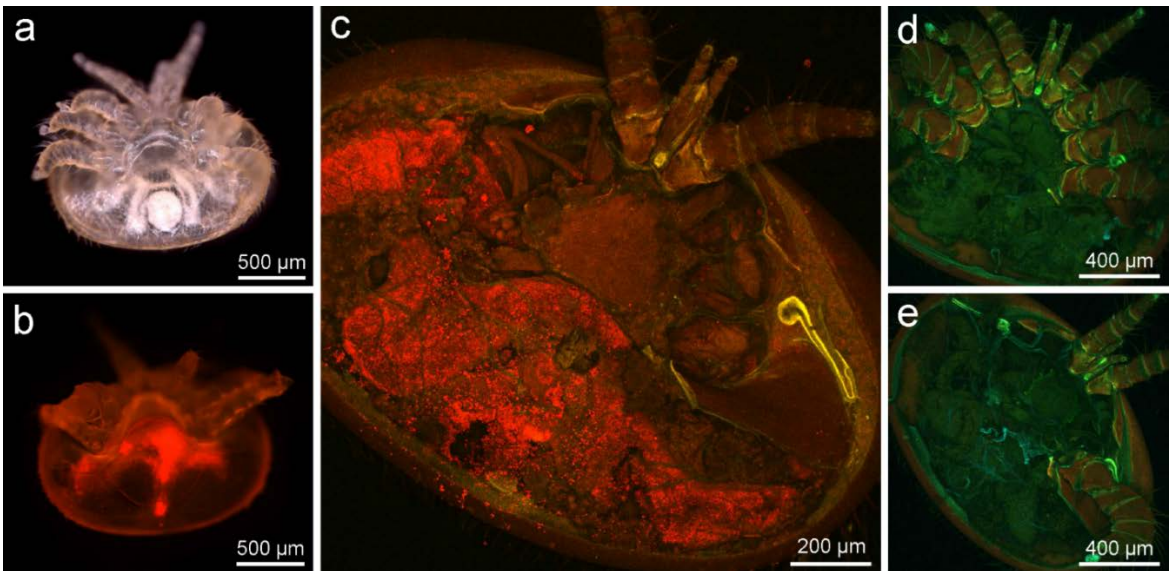


Figure 2.2

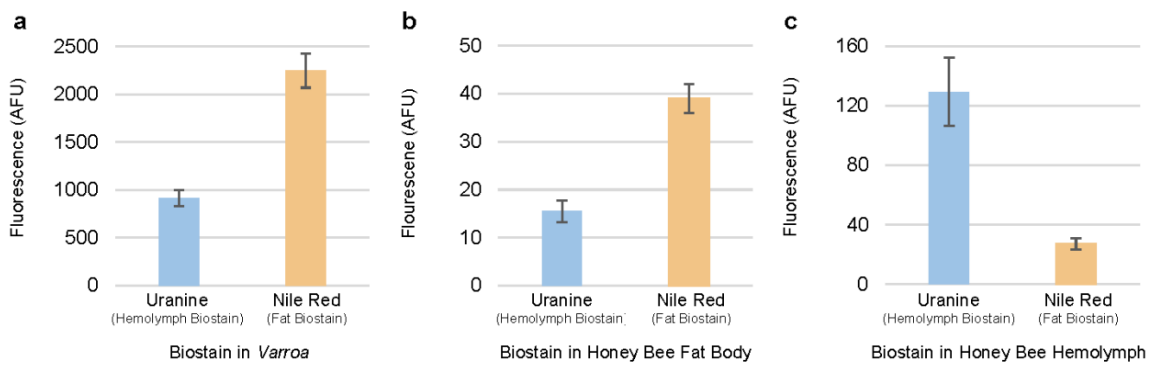


Figure 2.3

Figure 2.1 Host tissue collected from bees with fluorescently stained internal tissues showing the fidelity of each biostain (Nile Red and Uranine) for each host tissue (fat body and hemolymph respectively).

a-d, Hemolymph tissue shown in brightfield (**a**), and with fluorescent imaging (**b**). Fat body tissue shown in brightfield (**c**), and with fluorescent imaging (**d**).

Figure 2.2 *Varroa* fed on nurse bees with fluorescently stained hemolymph and fat body tissue primarily showed fluorescence associated with fat tissue.

a,b, *Varroa* after having innate fluorescence (autofluorescence) of the integument reduced via hydrogen peroxide bath (**a**). Bright red fluorescence (associated with fat body biostain) can clearly be observed in its multi-lobed digestive system without dissection (**b**). Note, fluorescence associated with the hemolymph (yellow) is very low and virtually indiscernible when imaged.

c,d,e, Confocal microscopy images of dissected *Varroa* fed only one of the fluorescent biostains. Mites fed on bees with fluorescently stained fat body show such high levels of Nile Red in the digestive system that the shape of the gut can be clearly observed via fluorescence imaging. Mites that fed exclusively on bees with biostained hemolymph (**d**) showed fluorescence only marginally above the control (**e**).

Figure 2.3 Mean biostain levels detected in *Varroa* and in biostain honey bee tissues. Fluorescence values reported in arbitrary fluorescence units (AFU).

a-c, Mean biostain levels detected in *Varroa* after 24 hours of exposure to stained host bees (**a**). Levels of the fat biostain (Nile Red) are higher than that of the hemolymph (Uranine) biostain and appear in the same proportion as in the fat body of the host bees (**b**), Proportion *Test* (*prop test*): ($\chi^2=3.62e-28$, $P=1$). This proportion differs significantly from that of the hemolymph of these bees (**c**) providing further evidence that mites are not consuming this tissue in significant amounts (*prop test*: $\chi^2=197.33$, $P<0.001$).

Discussion

Our results show that *Varroa* primarily consume fat body in their diet. This breaks from the accepted model that these mites are hemolymphagous. There has long been evidence in support of this conclusion. *Varroa* feeding reduces protein content in the metasoma of parasitized bees but not in the mesosoma, even at levels of 11 mites on one host (22). If *Varroa* are exclusively removing circulating hemolymph and, by consequence, the relatively low levels of protein in it, it is expected that the protein content in the mesosoma would also be reduced even if the mites are primarily withdrawing the hemolymph from the metasoma. However, the alternative model makes more sense of this observation as the removal of fat body tissue from the

metasoma would leave the protein content of the mesosoma largely unaffected. Further, mites fed on by *Varroa* show a notable disruption in their ability to replace lost protein, specifically in the metasoma (26). The removal of circulating hemolymph proteins could account for the reduced protein levels in the host but not the inability to replace them, however, feeding damage caused to the fat body likely would do so as it is the primary source of protein synthesis and storage in insects (47, 66-68).

The cells of the fat body synthesize the majority of the hemolymph proteins, storage proteins, lipophorin, antimicrobial peptides, and vitellogenins (47, 66, 67). Reduction in lipophorin and wax precursors, produced within specialized fat body cells called oenocytes, potentially accounts for the alterations to cuticular hydrocarbons and the dramatic water loss reported in multiple studies of *Varroa* parasitism in honey bees (22, 23, 25, 67). Several studies have shown that feeding by *Varroa* substantially decreases fat and protein content in adult bees and may even inhibit production of these molecules (16, 21, 22, 26, 69). Glinski (1984) (21) proposed that it was reasonable to assume that some other factor was at work in reducing protein concentrations in parasitized honey bees aside from the simple withdrawal of the hemolymph because protein reduction was still high in pupae parasitized by relatively few *Varroa*.

High metabolic activity is a defining characteristic of fat body tissue. It is the primary site of most of an insect's intermediary metabolism (47). As such, it is unsurprising that *Varroa* feeding decreases the metabolic rate of parasitized bees (22). Feeding interferes with the generation of precursor metabolites, oxidative phosphorylation, lipid metabolism and ultimately the production of biochemical

energy, an additional set of effects that were not accounted for within the conventional model (26).

Chapter 3: Determination of the Suitability of a Honey Bee Hemolymph or Fat Body Diet for Survivorship and Reproduction of *Varroa destructor*

Introduction

Both studies provide evidence that *Varroa* consume fat body tissue from adult honey bees. However, I also set out to determine if fat body is a dietary requirement impacting survival and fitness. To answer this question, I developed a bioassay which provided reproducing *Varroa* one of six host tissue diets with a hemolymph to fat body ratio of: 100%:0%, 75%:25%, 50%:50%, 25%:75%, 0:100%, and an unfed control. I monitored mites provisioned with the different diets for seven days, during which time I noted any oviposition and mortality.

Methods

Varroa for this study were taken directly from the sealed brood cells of heavily infested colonies maintained by the University of Maryland, College Park or the USDA ARS. Cells were selected that had been capped for approximately 12 hours. This length of time proved important as the mites appear to react to environmental cues that potentially induce transition into their reproductive phase during this period. In preliminary trials, mites removed prior to 12 hours produced very few offspring regardless of treatment. Significantly longer than 12 hours and the mite is likely to begin feeding on the developing prepupa. The end of this period is marked by the initiation of the cocoon spinning phase thus larval age could be estimated accurately based on the presence of silken fibers lining the underside of the capping. The results

of this study could potentially be biased if some *Varroa* were able to feed on host brood prior to the trial. This would afford the individual mites different nutritional starting points at the outset of the trial.

Brood cells were opened by removing the wax capping using dissecting tools. Foundress reproductive mites were transferred to artificial enclosures and given 20 μ l of honey bee tissue through an artificial membrane. Survivorship was recorded once per day over the course of 7 days. At the start of the trial, each foundress mite was introduced into her own artificial enclosure, a standard commercial queen cup made of compressed wax. Inside of each cell, I introduced one size five gelatin capsule containing the treatment solution. Size five gelatin capsules are 1.1 cm in length, about the size of an average 5th instar worker bee larva and functioned well as “decoy larva” for this experiment. A large section of the gelatin capsule was cut away and replaced with Parafilm stretched by hand to between 10 and 15 μ m. Bruce et al. (1988) (70) showed that mites were able to feed through a membrane of this thickness. Live prepupae were pressed against the parafilm membrane to transfer cuticular semiochemicals onto the surface of the membrane to stimulate feeding in foundress mites. Parafilm was used to coat the outside of the cell to give a similar consistency to that of soft larva. As a wax product, parafilm adheres very well to the surface of other wax products, thus to hold the pill in place, I pressed the parafilm coating the outside of the pill against the roof of the wax enclosure. The inside of the cell was wrapped in parafilm as well to avoid the pill dissolving when exposed to the diet. The foundress mite (and any offspring) were allowed to feed ad libitum through this membrane for the duration of the trial. The contents of the capsule were filled once every 24 hours by

piercing the wall of the capsule with a hypodermic needle and injecting the treatment solution into it directly. Artificial cells containing the foundress mite and the decoy larva were pressed into standard microcentrifuge tube racks and placed in an incubator at 34°C and 70% RH.

Five foundress mites were randomly assigned to each treatment per trial. Treatment solution consisted of 1 of the following formulations: 75% hemolymph to 25% fat body, 25% hemolymph to 75% fat body, 50% hemolymph to 50% fat body by volume, 100% hemolymph, or 100% fat body in DPBS (Dulbecco's phosphate buffered saline to function as a carrier mimicking the salinity and pH of insect hemolymph). Hemolymph was collected from nurse bees and transferred into pills using Hamilton Gastight Chromatography Syringes. Fat body tissue for this trial was dissected from the same nurse bees. While immature bees are the natural host of gravid *Varroa*, the distribution of fat body cells as a free floating mass throughout the hemolymph made it prohibitively difficult to adequately separate the two tissues for a clear assay. Adult fat body was used because it is a connected mass localized to the inner dorsal surface, and to a greater extent, the inner ventral surface of the metasoma. After removing the digestive system, and wicking away excess fluid, fat body tissue was removed using fine forceps. This tissue was liquefied using a Polytron PT 1300D hand-held tissue homogenizer. and transferred into the pills using Hamilton Gastight Chromatography Syringes. Nurse bees were collected directly from the brood nest of several colonies tended by the University of Maryland, College Park. In addition our diet relied of fat body from adult honey bees.

Results

Mites that were provisioned with hemolymph only survived 1.8 ± 0.8 days on average with 5% producing eggs which was not different from the group that was starved, living 1.3 ± 0.64 days with 0% fecundity (Figure 3a-c). As the concentration of fat body in the diet increased, survivorship and egg production increased as well ($r^2=0.9634$) (Figure 3d). Mites given no hemolymph, only fat body, showed the highest average rate of survivorship (3.5 ± 1.5 days) and fecundity (40%) to those fed all other diets (Figure 3a-c). Only mites in the 100% fat body or 50% fat body treatment survived the full 7-day length of the experiment, albeit in relatively low numbers (20%). Mites provisioned with 100%, 75% and 50% fat body in their diet had the highest fecundity rates respectively 40%, 20%, and 32%. The diet composed of 25%:75% hemolymph:fat body contributed far more rapidly to the growth of fungus than the other diets and as such, a disproportionate number of experimental units were lost, likely contributing to the lower than expected survivorship and fecundity in this treatment.

The rate of egg production for mites on our most successful diet – 100% fat body (40% fecundity), was lower than the rates documented in natural conditions (varying between 60% and 90% in worker brood based on factors that are yet undetermined(5, 71). The low fecundity rates and relatively low survivorship are likely explained by the artificial nature of this laboratory study.

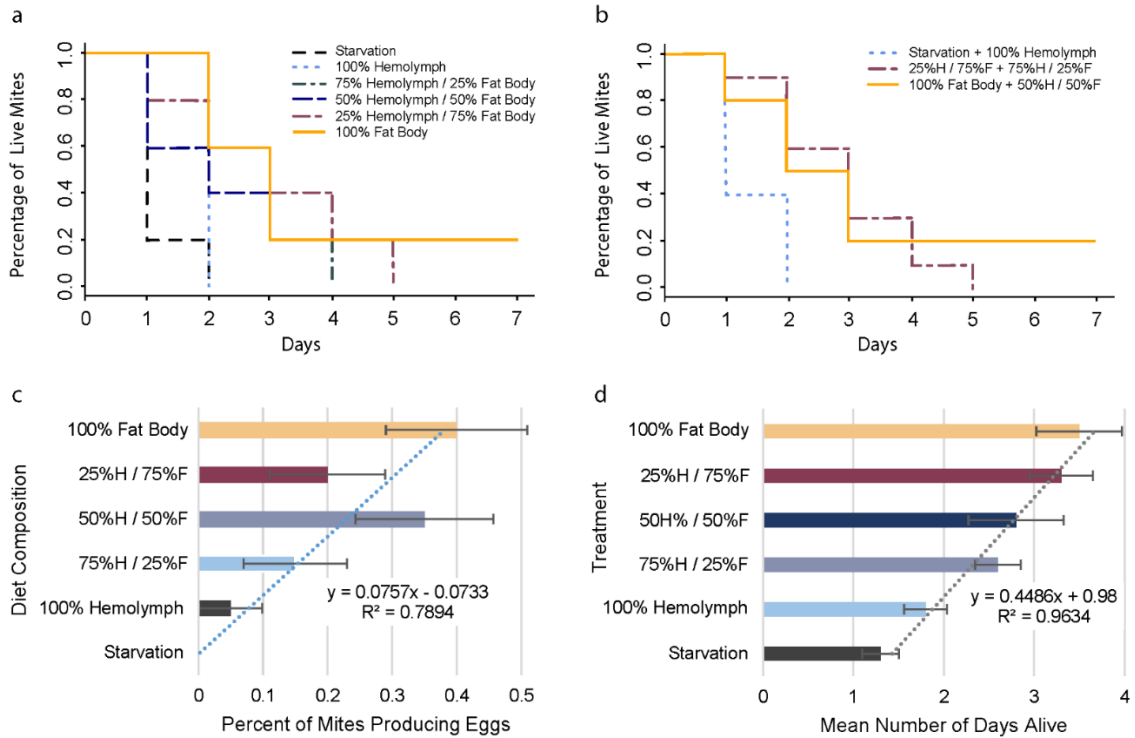


Figure 3

Figure 3 Mites fed honey bee fat body tissue survived longer and produced more eggs than mites provisioned hemolymph. High mortality was observed across treatments; likely owing to the artificial setting. After 3 days, mites receiving 0%:100% and 25%:75% hemolymph:fat body as their diet maintained survivorship at 60% while the 100%:0% hemolymph:fat body and the starvation control had already exhibited full mortality.

a,b, Survivorship curve showing starvation control and all five host tissue diets (**a**). **b**, represents the same data with levels combined that show no difference in survivorship. Note, mites provisioned hemolymph and mites given no food showed no difference in survivorship. However, survivorship differed substantially between the hemolymph treatment and all treatments given any level of fat body ($\chi^2= 16.1$, $P<0.001$).

c, Average survivorship of mites differed by diet. Survivorship and the ratio of fat body by volume adhere to a strong positive linear relationship ($R^2=0.9634$).

d, Egg production differed between treatment diets (ANOVA: $P<.004$). A positive linear relationship was observed between egg production and the amount of fat body in the diet of the mite ($R^2=0.7894$).

Discussion

These findings provide sufficient evidence to reject the conventional model that *Varroa* are hemolymphagous parasites. The location of their feeding site, the pre-digested fat body cells therein, the presence of lipid-dense host tissue in the gut of the

mite, and the strong relationship between survivorship, fecundity, and the levels of fat body in the diet of the mite all suggest that the primary host tissue consumed by *Varroa* is the fat body. This fundamentally changes our understanding of this agriculturally significant parasite and has important implications for bee researchers attempting to understand the etiology of varroosis. The development of tools, both chemical and nonchemical, to manage this pest is particularly likely to be affected by these findings. The *in vitro* system used in this study is the first to maintain *Varroa* off-host for more than a week. With further refining of diet and culture conditions it may be possible to rear mites for the full 12-14 day period of their reproductive cycle in capped cells, contributing useful insight into the intricacies of and potential vulnerabilities in their lifecycle. These findings further help to explain why past attempts to develop *in vitro* *Varroa* rearing models have failed (70)(72), as they attempted to use diets based on the nutritional content of honey bee hemolymph rather than fat body tissue. Similarly, lack of success in developing effective systemic pesticides likely owes to the same issue of tissue misidentification (16). It was considered fact at the time of their development that mites fed on hemolymph, thus these pesticides were likely formulated to persist in the hemolymph of the honey bee rather than the fat (16). These findings have practical implications for the development of novel *Varroa* management technologies such as systemic RNAi which would need to be formulated to accumulate in fat tissue to target this parasite.

These results mark an advancement in our understanding of exactly how *Varroa* feeding impacts honey bees on both the colony and individual level. *Varroa* parasitism is associated with impaired development of immature bees (22), decreased lipid

synthesis (22), reduced protein titers (22), desiccation (25), impaired metabolic function (22, 26), inability to replace lost protein (26), precocious foraging (73), heightened winter mortality (74), impaired immune function (27, 28), decreased longevity (16, 74), and reduced pesticide tolerance (75). This diverse array of pathologies was difficult to account for under the conclusion that the parasite is feeding on hemolymph but is well explained by exploitation of the multi-faceted fat body tissue. The fat body facilitates metamorphosis, regulates metabolism, plays an integral role in both thermoregulation and osmoregulation and it synthesizes and stores lipids and proteins (47, 66, 67). The role of the fat body in protein synthesis accounts for early task shifting and impaired immune function as the fat body produces vitellogenins which are essential in signaling task shifting as well as antimicrobial peptides for proper immune function (47, 73). Evidence of extra-oral digestion in this study provides further weight to the finding that a significant volume of apparent salivary content is left behind after *Varroa* feed (22). How long this material remains bioactive is not yet known but likely extends the impact of feeding beyond the volume of tissue directly consumed by the feeding mite.

Fat body tissue also plays a crucial role in pesticide detoxification by absorbing and sequestering a wide range of xenobiotics thereby preventing them from finding their active site and causing damage (67, 76). Recent studies have shown that honey bees fed upon by *Varroa* suffer damage from pesticides even at concentrations that previously would have been inert suggesting that their feeding on this tissue may disrupt the process of pesticide detoxification (75). This factor potentially plays a role in the observed honey bee health decline considering the near ubiquitous presence of

Varroa in honey bee colonies and the heavy reliance globally on chemical pesticides. Exploitation of this pathway as a novel miticide delivery strategy may be possible if a miticide tolerable to the bees can be incorporated into the bees feed to be subsequently absorbed by the fat body during digestion and delivered to the mites when they consume this tissue during the dispersal phase.

Healthy fat body tissue is also critical to overwintering success; thus, these findings underscore an imperative for beekeepers to reduce *Varroa* populations in colonies prior to the emergence of so-called “winter bees”. Simple reduction of mite load late in the season may not be enough as vitellogenin produced by and stored in the fat body reduces oxidative stress substantially extending the lifespan of the bees during the winter (73, 74). Impairment of this function is expected to adversely impact winter survival and spring build up. Removal of fat body tissue from winter bees developing below the capping would also disrupt the process of metamorphosis. As enzymes disintegrate the juvenile organs, those macromolecular components are absorbed and slowly released by the fat body to structure the adult organs (50). Removal of fat body tissue during this critical process would ostensibly have implications for the eventual size and health of the adult insect. Treatment would likely be more effective in late summer or early fall before mites can significantly damage fat body tissue in winter bees. The ability of this parasite to negatively affect such a broad array of processes further highlights the critical link between this parasite and honey bee health. Our work reflects a need to reexamine even the fundamentals of our knowledge of *Varroa* as I work to diminish its impact.

Chapter 4: Reproductive Protein Stealing in *Varroa destructor*

Introduction

Varroa destructor is the causative agent of more honey bee pathologies than any other single factor affecting honey bee populations globally (4, 5, 77). How feeding leads to a number of these pathologies is still poorly understood (5, 22, 23, 25, 27, 59, 74, 78). In addition, the rapid reproductive capability of this parasite is remarkable and has been the subject of several studies (16, 79-86). Among the most notable observations is the ability the foundress mite to produce an egg constituting a sizeable portion of her body volume every 30 hours (81, 83).

The recent finding that this parasite feeds on host fat body, a multifaceted organ involved in several functions, suggests that these two observations may be linked. One key feature of the fat body in honey bees is that it is the synthesis and storage site of the vitellogenins, the precursors of egg yolk in oviparous organisms. By feeding on pupal fat body, *Varroa* are able to exploit a predigested, abundant, nutrient dense tissue during a segment of their life cycle that is defined by strong evolutionary pressure to quickly produce as many offspring as possible or, in the case of immature mites, to grow as quickly as possible. The ability to use a tissue that already holds the class of proteins that eggs need for proper development likely streamlines this process further.

Varroa reportedly have the ability to pass certain proteins through their digestive tracts undigested consistent with the finding that these parasites have little to no enzymatic activity in their midgut (16). More intriguing still is a finding that has

gone largely unexplored, the presence of host proteins in the eggs of *Varroa* (87). No one has yet determined the identity of these proteins or the origin of these proteins within the host. Tewarson (1982) (87) speculated that because the *Varroa* is depositing these proteins into its eggs, that this parasite is using them as its vitellogenins. Knowing that *Varroa* are feeding on the tissue that produces and stores them in the bee raises the possibility that this parasite is actually siphoning vitellogenins directly from host bees and depositing them into its own eggs. This would be the first described instance of a parasite stealing reproductive proteins from its host to be used for the same function in its own lifecycle. This reproductive protein kleptoparasitism would represent a markedly efficient and evidently fine-tuned mode of host exploitation. The term kleptoparasitism (literally “parasitism by stealing”) is typically used when one organism steals a food resource from a host. This circumstance differs in that the resource, though derived from digested food, is a molecular component of the host. Nonetheless, I would contend that the ecological impact is the same; the host is deprived of a nutritional resource that the parasite is then able to use for its own purposes. I would contend, that the term should be used to describe this instance as well.

In this study, I used polyclonal antibodies developed to react to honey bee vitellogenins as a means of identifying a honey bee protein found in *Varroa* eggs. Confirmation was undertaken via high performance liquid chromatography mass spectrometry.

Methods

Sample Collection for Protein Assay

Samples were collected from queen right colonies in College Park, Maryland and Oviedo, Florida. Frames were collected from the brood nest, capped cells unsealed using insect dissection tools, and white-eyed brood removed from 30 cells. Three white-eyed drone pupae and three white-eyed worker pupae were used to create pooled fat body/hemolymph samples. To collect internal tissue each specimen was secured using four insect pins at the base of the prosoma and mesosoma. A shallow cut was made along the lateral margin of the metasoma where the sternites and tergites meet and another incision across the anterior ventral margin of the metasoma. The metasoma was then opened, pinned down, and the digestive system removed using a micropipette. Comingled fat body and hemolymph tissue were then collected using a micropipette. Freshly laid honey bee eggs were identified based on their upright posture in the cell and 28 collected using a soft paint brush.

18 Gravid adult mites and 28 mite eggs were collected from unsealed brood cells as well. Gravid females were identified based on separation between the dorsal shield and anal sclerites. Distinct separation between them visible from the posterior end of the mite and taut interscutellar membrane have been noted in previous observation by dissection as clear indications of mid to late stage vitellogenic oocyte development. Mite eggs were collected in similar manner to honey bee eggs using a soft paint brush. Egg samples from both honey bees and mites were handled as little and as carefully as possible to avoid damaging the soft chorion thereby introducing exogenous proteins and other contaminants.

Each group of tissue samples was transferred to a microcentrifuge tube with 100µl of lysis buffer and tissue disruptor beads. A *FastPrep-24 5G Benchtop Homogenizer* was set to a 2 minute cycle to achieve adequate membrane disruption and homogenize each sample. The samples were centrifuged for 3 minutes at 13,000 rpms. The protein content of each sample was determined using a *NanoDrop 8000 Microvolume UV-Vis Spectrophotometer*.

Protein Separation via Gel Electrophoresis

Samples of hemolymph/fat body homogenate from drone pupa, worker pupa, homogenate of honey bee eggs, full body homogenate of gravid *Varroa*, and homogenate of *Varroa* eggs were run on *NuPage 4-12% Bis-Tris Reducing Protein Gels (Thermo-Fisher)* in an *XCell Surelock Mini-Cell Electrophoresis System (Thermo-Fisher)*. The respective volumes of distilled water and sample homogenate were adjusted to bring each sample to 50 µg/µl per lane. Six grams of a molecular weight marker were added in the right most lane. An identical gel was run on the opposing side of the buffer chamber in the *XCell Surelock System* to allow for western blot analysis of one gel and Coomassie staining for mass spectrometry of the other.

Vitellogenin Identification via Western Blot

Immediately upon completion of the gel run, one of the two identical gels was prepared for western blot. Using the same *XCell Surelock System*, separated proteins were transferred to *Invitrolon PVDF Membrane (Invitrogen)*. The membrane was then placed in blocking solution and allowed to incubate facilitated by a rotary shaker for 30 minutes. The membrane was then washed with *UltraPure DNase/RNase-Free*

Distilled Water and incubated further with 10ml of a custom polyclonal antibody against honey bee vitellogenin (*Pierce Custom Antibodies*) for 1 hour on a rotary shaker. The membrane was washed with *Antibody Wash (Invitrogen)* according to manufacturer recommendations and incubated in *Secondary Antibody (Invitrogen)* for 30 minutes. The *Secondary Antibody* solution was decanted and after further washing by manufacturer recommendation, 5ml of *Chromogenic Substrate (Invitrogen)* was added until bands were visible.

Vitellogenin Confirmation via HPLC-MS/MS

Bands identified via western blot were excised from the corresponding duplicate gel using a feather blade and were submitted to the University of Maryland Proteomics Lab for further identification. Proteins were dissolved in 6M guanidine HCL and subsequently heated to 95°C for 20 minutes. The reaction was allowed to cool and for the native gel, 50 mM Tris HCl was added until the guanidine HCl concentration was less than 1M. The native proteins were dissolved in a 7.5 pH buffer solution. Trypsin Gold was added for a final protease:protein ratio of 1:100 to 1:20 and the protease/proteins incubated at 37°C for one hour. An aliquot was removed and the mixture frozen at -20°C.

Post-digestion, protein samples were analyzed using a *ThermoFisher Orbitrap Fusion Lumos Tribrid Mass Spectrometer* interfaced to a *Dionex UltiMate 3000 RSLCnano HPLC System*. A linear gradient of water to 50% acetonitrile running at 250 nl/min was used to elute the peptides from the column.

Results

Protein Separation via Gel Electrophoresis

Samples of hemolymph/fat body homogenate from drone pupa, worker pupa, whole honey bee egg homogenate, whole *Varroa* egg homogenate, and full body gravid *Varroa* homogenate were run via reducing SDS gels. When run on an SDS gel, a clear band was present in the region of 180 to 220 kDa for the *Varroa* mite eggs and all other tissue samples (Figure 4.1 a). This band corresponds to the reported size of the full-length honey bee vitellogenin (180 kDa). Because the molecular weight marker is only able to estimate the weight of a protein within a 15% margin of error, I could not determine the exact molecular weight. This band was stained especially intensely in the honey bee egg sample. After honey bee eggs, this band presents most intensely in the eggs of the mite. A clearly defined band was also detected at about 40 kDa potentially corresponding to a vitellogenin fragment found only in fat body tissue. No band is present for the corresponding 150 kDa fragment resulting from the cleavage of the full length vitellogenin. Several other bands appear consistently across samples implying that multiple proteins aside from vitellogenins are being siphoned from the host pupa by the foundress mite and are being conveyed to the developing oocyte. Nearly all, if not all, of the recognizable bands present in the gravid mite show up in the lane for the mite egg as well.

Vitellogenin Identification via Western Blot

The western blot confirmed the presence of honey bee vitellogenin in the region of 180 to 220 kDa across all samples including the eggs of the *Varroa* mite (Figure 4.1

b). The entire bee egg lane reacted with marked intensity darkening its whole length. However, several distinct bands can still be resolved. The region of highest intensity is at about 200 kDa and above. A well-defined band was also detected in the region between 55 and 35 kDa as expected for the 40 kDa vitellogenin fragment. This second band was also shared across samples fragmenting into two closely associated bands in the gravid mite lane and three in the mite egg lane.

Vitellogenin Confirmation via LC-MS/MS

Preliminary data provided via mass spectrometry supports the information provided by the immunological techniques. Honey bee vitellogenin was detected in the gravid mites, mite eggs, and all honey bee samples. A vitellogenin fragment of about 44.5 kDa was also identified across samples corresponding to the second conserved band in the western blot. Both of vitellogenins of *Varroa* were also found in the eggs and body of the gravid female.

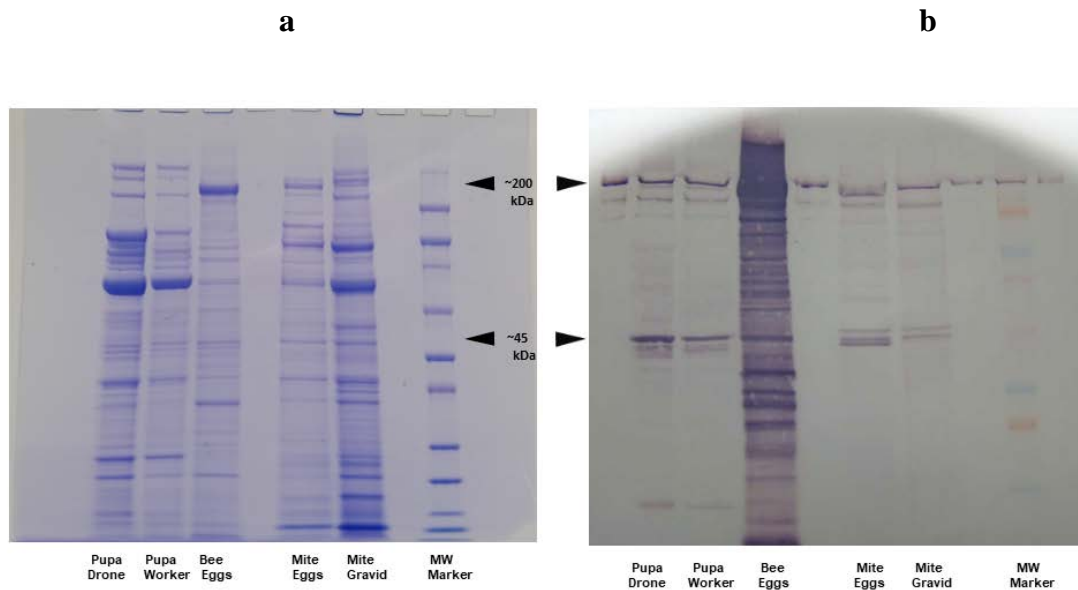


Figure 4.1

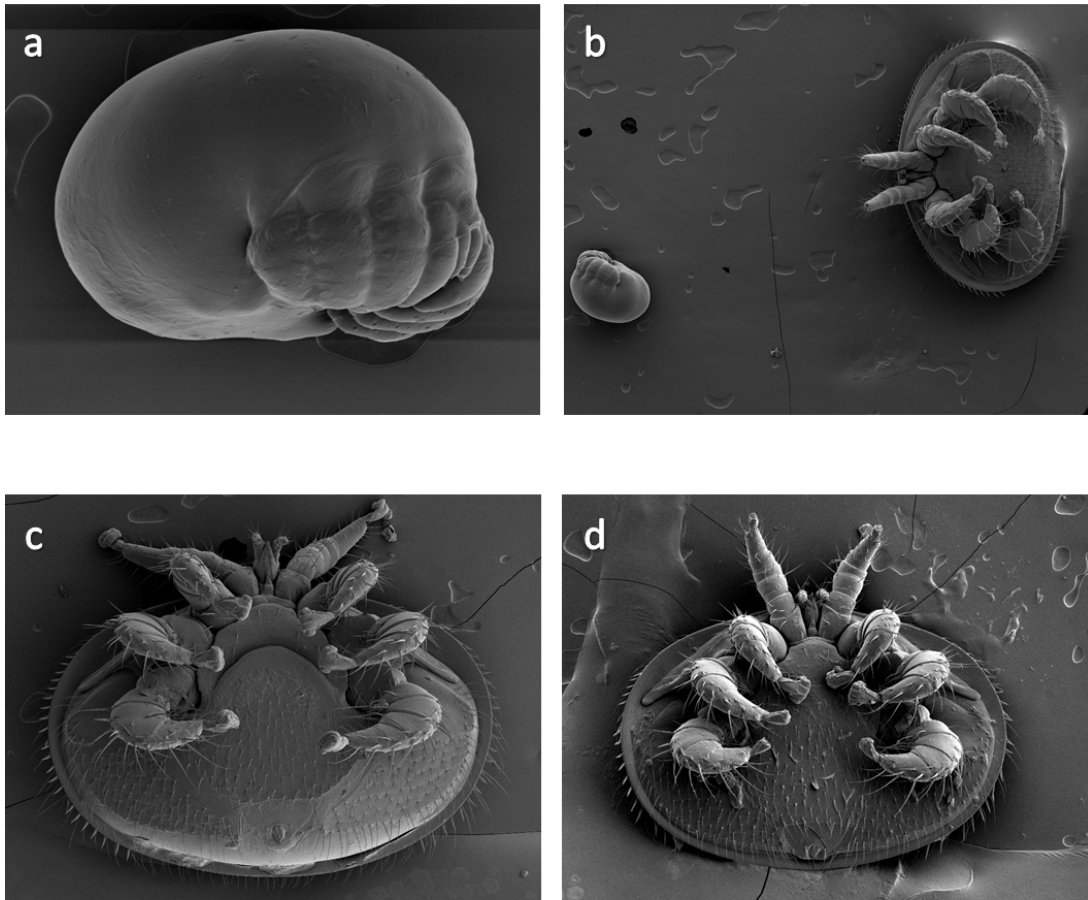


Figure 4.2

Figure 4.1 SDS reducing gel and associated western blot comparing proteins present in mite and honey bee tissues. Lane 1 is blank, followed by a pooled sample of hemolymph and fat body from white-eyed drone pupae, hemolymph and fat body from white-eyed worker pupae, homogenate of honey bee eggs, blank, homogenate of *Varroa* mite eggs, full body homogenate of gravid *Varroa* mites, blank, and a molecular weight marker.

a, SDS reducing gel showing several proteins present in different honey bee and *Varroa* mite tissues. Note the well-defined, conserved bands of the molecular weight corresponding to honey bee vitellogenin and cleaved fragment found only in honey bee fat body tissue.

b, Western blot identifying vitellogenin at two distinct molecular weights using a custom polyclonal antibody. These bands correspond to the full-length fragment of vitellogenin just

below 200 kDa and the N-terminus fragment just above 40 kDa. As is to be expected the honey bee egg produced the most intense immunological response to the antibody with vitellogenin and the biochemically similar vitellin being the primary constituents of early stage eggs.

Figure 4.2 Details of *Varroa* reproduction studied via LT-SEM. Late stage gravid *Varroa* produce an egg comprising a substantial portion of their body volume every 30 hours representing an accelerated reproductive capacity. The volume of the developing oocyte is so large that it results in conspicuous differences in appearance between late and early stage gravid females.

a, b, showing fine details of a *Varroa* egg at 200x (**a**) and a size comparison between an egg and a gravid female 40x (**b**). The egg is oviposited by the female with an already well-developed protonymph inside. Note the distinctive imprint of legs and palps visible through the thin chorion.

c,d, Oviposition is imminent for the female imaged in panel (**c**); a state characterized by a generally bloated appearance and taut interscutellar membrane most conspicuously visible posterior to the anal plate. Compare with panel (**d**) in which the female shows appearance characteristic of early stage or suspended oocyte development.

Discussion

Our results strongly suggest that *Varroa* are not only ingesting host vitellogenins but also conveying them to their eggs undigested. Furthermore, all three forms of analysis identified both the full-length 180 kDa vitellogenin molecule (which is present in fat body tissue and hemolymph) and an abundant approximately 40 kDa fragment (present only in fat body tissue). This fragment is produced by cleavage of the 180 kDa monomer; a proteolytic process occurring only in the non-circulating, parietal fat body located in the metasoma (68, 88). These findings are consistent with the findings of my previous work showing that *Varroa* feed primarily on fat body tissue.

It has already been noted that the rapid rate of reproduction characteristic of the *Varroa* lifecycle requires adaptations to accelerate normal processes (81, 87). Considerable development of the immature mite takes place inside of its mother to the extent that a single developing ovum takes up most of the internal space of the female before oviposition (Figure 4.2). Gestating offspring this advanced in development

clearly requires a substantial input of biochemical energy, a demand met by host vitellogenin. I was able to identify both vitellogenins of the mite in their eggs as well, suggesting that host vitellogenin is used as a supplementary means to accelerate their reproduction and development to meet needs posed by the impending uncapping of the cell.

This reproductive strategy prompts comparison with the tsetse fly (Glossinidae, Diptera). This organism has similar needs to *Varroa* and has been shown to employ a similar strategy to meet them (89). These flies gestate a single juvenile beyond the hatching of the egg, through larval development, eventually producing a large late-stage larva the way that most other insects lay clusters of eggs. This developmental strategy, employed broadly in this fly and closely related flies, allows the juvenile the entirety of its nutrition from its mother until adulthood (90). Likely as a means to meet this constant and very substantial nutritional demand, the tsetse flies are able to move large proteins undigested across the membrane of the midgut avoiding the energetically taxing task of protein catabolism (89). A closer relative of *Varroa*, the tick (Ixodidae, Parasitiformes), is known to share this capability as well (91).

These findings not only provide a model for understanding accelerated reproduction and development but a model for better understanding *Varroa* associated pathologies. *Varroa* feeding is linked to early task shifting, faster worker senescence, reduced immune function, and overwinter failure as should be expected (5, 74, 92, 93). Parasitic feeding would reduce the honey bees access to these critical molecules that honey bees depend on as a regulatory molecule for timely task shifting, a means of reducing oxidative stress, as an essential immune system component, and as a diverse

source of sustenance during winter when only a simple diet of carbohydrates is available (74, 88, 94, 95).

As vitellogenins are integral to winter survival these findings provide further imperative to beekeepers to keep *Varroa* levels low in late summer/early fall when winter bees are being produced. Further, attention should be paid to fall treatment to reduce the over-winter mite load. It is likely that these parasites continue feeding during this period and, in so doing, they compete with the honey bees for a vital resource that they are unable to replace.

The most abundant protein in *Varroa* is a large lipid transfer protein but contrary to what may be intuitive, it is far more abundant in the dispersal phase rather than the reproductive phase (84). In light of our findings, the presence of this lipid shuttle protein is likely an adaptation for surviving the winter. The ability of *Varroa* to steal the honey bee's reproductive protein for its own reproductive needs suggests potential for this parasite to adopt the adapted uses of this protein as well. This is likely the means that short-lived *Varroa* extend their lifespan through the winter as well.

In future study of this system, I propose utilization of fluorescent staining techniques to trace the movement of this large molecule from the honey bee fat body, through the digestive system, the hemolymph of the mite, potentially the lyrate organ, to its final destination within the developing oocyte. I would also like to explore methods of determining the ultimate fate of vitellogenins consumed by dispersing mites. There is potential that these valuable proteins are shuttled by LLTP to the lyrate organ or fat body of the mite to be used during periods of starvation (i.e. winter) or as reserves for the reproductive process.

Chapter 5: Morphology of *Varroa destructor* Detailed Via Low-Temperature Electron Microscopy with Emphasis on Variable Characters

Introduction

Over millions of years of evolutionary time, four genera *Acarapis* (Tarsonemidae, Prostigmata), *Tropilaelaps* (Laelapidae, Mesostigmata), *Euvarroa* (Varroidae, Mesostigmata), and *Varroa* (Varroidae, Mesostigmata), have developed intimate associations with honey bees to the extent that they cannot exist apart from them. The *Acarapis* have modified setae and ambulacra adapted for both endo and ectoparasitism of adult bees (96). The *Tropilaelaps* have a body plan that apparently sacrifices efficient exploitation of adult bees for further specialization in brood parasitism (97). However, the *Euvarroa* and *Varroa* are well suited to the exploitation of both adult and immature bees owing to a number of morphological adaptations (64, 98, 99). These anatomical structures have been studied with multiple preparations and imaging techniques, all of which are prone to leave behind artefacts that can obfuscate important characters (7, 38, 42, 100-106). To this point, no morphological differences have been determined between *V. destructor* and its closest relative *Varroa jacobsoni*. The two were considered the same species for decades before being resolved on a genetic basis (7). The only distinction used to distinguish between them has been a relatively small difference in size with *V. jacobsoni* being smaller than *V. destructor* (7).

While conducting a previous study, I collected an exceptionally small specimen of *V. destructor*, far smaller than the smallest recorded *V. jacobsoni* (7). This specimen was confirmed to be *V. destructor* via genetic analysis calling into question whether identification based on size is reliable. The collection of further specimens below the size range of *V. destructor* revealed a need to update our understanding of *Varroa* morphology and to determine morphologically distinct features that can be used to distinguish between seemingly cryptic species. To do this, it is, I set out to eliminate the aforementioned artificial alterations to the appearance of *Varroa destructor* using low temperature scanning electron microscopy (LT-SEM).

One of the defining qualities of the Acari is the diminutive size of these chelicerates, hence the name “mites”. As such, microscopy is an indispensable tool in acarology. Though *Varroa* are relatively large for mites, it is still often prohibitively difficult to accurately resolve key characters with the unaided eye or even light microscopy. Acarologist Oudemans had difficulty determining the nature of the cheliceral digits in 1904 when he described the genus *Varroa* as having no upper digit with the lower digit fixed. To the contrary, the upper digit is greatly reduced but is still present and what he referred to as a “fixed under-jaw” is a fully mobile digit. Further, the usage of preparation techniques such as critical point drying to remove liquid from samples (used in scanning electron microscopy studies of *Varroa*) causes the shrinkage and general distortion of tissues that can limit the usefulness of SEM as a method of describing the finer details of delicate structures (107, 108).

By contrast, no preparation is necessary for LT-SEM. Active specimens are instead immersed in liquid nitrogen immediately arresting all biological processes. This

effectively freezes the sample in time for further critical analysis. This method has provided the means for further detail in description of fine morphological characters in *V. destructor* and the potential for determining differences between this species and its cryptic species *V. jacobsoni*. The presence of two distinct, and normally geographically isolated, haplotypes of *V. destructor* in the US points to multiple introductions of this parasite into the Americas suggesting the potential for further introduction of *Varroa* species or haplotypes in the future (7, 11, 109). With no identified morphological differences between them, researchers are reliant on time-consuming DNA evaluation methods that require the specimen to be damaged or destroyed for positive identification. Distinguishing between species via morphology would provide researchers another tool to verify that only one species within the *V. destructor-jacobsoni* cryptic species complex exists in the US. Attention to fine morphological details has also revealed important information as to how the unique morphology of *V. destructor* facilitates such efficient host exploitation.

V. destructor is the larger of the two measuring 1.17 by 1.71mm on average. *Varroa jacobsoni* measures 1.06 by 1.55mm on average. The adult female of both species is dark red in color. The idiosoma is covered entirely by a convex dorsal shield that is ellipsoid in shape being wider than long. The attachment points of the appendages of the mite are obscured by this protective shield when viewed from above. The venter of the mite is comprised of eight discrete sclerites: the exapodal, sternal, genital, a pair of anterior metapodal, a pair of posterior metapodal, and the anal sclerite. The intervening membrane is called the interscutellar cuticle. A number of characters such as sensillus placement, peritreme dimensions, and, to some extent, chaetotaxy

(arrangement, size, and number of hairs on an organism) have been of use in distinguishing between other *Varroa* species. These characters will receive greater focus in this study as will features found to differ from all previous descriptions of *Varroa*.

Methods

Samples of apparent *V. destructor* were collected in two regions of the US, the North and South represented by Maryland and Texas respectively. US samples were collected throughout the summer and fall from managed colonies in College Park, Maryland and College Station, Texas. Samples in South and Southeast Asia were collected in Gazipur, Bangladesh and Chiang Mai, Thailand during the hot and wet seasons. Specimens not fitting with the description of *V. destructor* as provided by Anderson and Trueman (2000) (7) and de Guzman (1999b) (110) were sent to the USDA for sequencing to determine species and haplotype. Mites of varying life stages were collected from brood and adult bees. Mites on adult bees were removed using a fine paint brush or left in place on the bee for analysis of the parasite on host. Specimens in brood were collected by removing the wax capping on sealed cells using dissecting tools. The foundress mite, male, and any immature mites were removed with a fine paint brush.

The majority of the samples were placed in liquid nitrogen while still living but this was not always possible with some of the samples collected outside of the US. These samples were placed in empty microcentrifuge tubes and placed in a styrofoam container with dry ice. Where dry ice was prohibited by airline transit standards, other samples were deposited in microcentrifuge tubes with alcohol and placed in -20°C *Nalgene Labtop coolers*. These samples were placed directly in liquid nitrogen upon removal from alcohol in the US. Low temperature scanning electron microscopy was conducted at the USDA ARS Electron and Confocal Microscopy Unit using techniques outlined by Bolton et al. (2014) (49). Mites were secured to 15 cm x 30 cm copper plates using ultra smooth, round (12mm diameter), carbon adhesive tabs (Electron Microscopy Sciences, Inc., Hatfield, PA, USA).

The specimens were frozen conductively, in a Styrofoam box, by placing the plates on the surface of a pre-cooled (-196°C) brass bar, the lower half of which was submerged in liquid nitrogen (LN₂). Other specimens were frozen via the same means, on the surface of the host. After 20-30 seconds, the holders containing the frozen samples were transferred to a Quorum PP2000 cryo-prep chamber (Quorum Technologies, East Sussex, UK) attached to an S-4700 field emission scanning electron microscope (Hitachi High Technologies America, Inc., Dallas, TX, USA). The specimens were etched inside the cryo-transfer system to

remove any surface contamination (condensed water vapor) by raising the temperature of the stage to -90 °C for 10-15 min. Following etching, the temperature inside the chamber was lowered below -130 °C, and the specimens were coated with a 10nm layer of platinum using a magnetron sputter head equipped with a platinum target. The specimens were transferred to a pre-cooled (-130 °C) cryostage in the SEM for observation. An accelerating voltage of 5kV was used to view the specimens. Images were captured using a 4pi Analysis System (Durham, NC).

Results

As a part of this study, 484 images were captured of 71 apparent *V. destructor* specimens from the US and Asia. The usage of LT-SEM allowed for the capture of images showing specimens posed as they were when living and preservation of key characters in their natural shape and conformation. No consistent physical differences were found between populations of mites in the size range of *V. destructor* in the US and those in Asia. However, several, thus far unreported, differences were observed between these mites and previous descriptions of them.

Further, one specimen was collected in Maryland showing substantial differences in size and shape from the archetypical structure of *V. destructor*. This specimen was rounded rather than being distinctly wider than long. It measured 9.92 by 1.23mm, measurements significantly smaller than even *V. jacobsoni* (Figure 5.1). This was the only specimen collected that lacked the seta posterior to the anus (post-anal seta). This individual also had a far more distinct cribrum than all of other specimens collected in this study and an anal plate with a shape more pentagonal than the typical triangular shape. The specimen was smaller than the smallest recorded *Varroa jacobsoni*. This specimen was, however, determined to be *V. destructor* albeit an extremely atypical representative of the species. The haplotype of this specimen is yet undetermined. It was collect from a colony in which another specimen was retrieved

that was significantly smaller than *Varroa destructor* as well (though morphologically similar in most other respects) (Figure 5.1). This suggests that there is far greater phenotypic plasticity and associated morphological variability in *V. destructor* than previously noted and warrants further study.

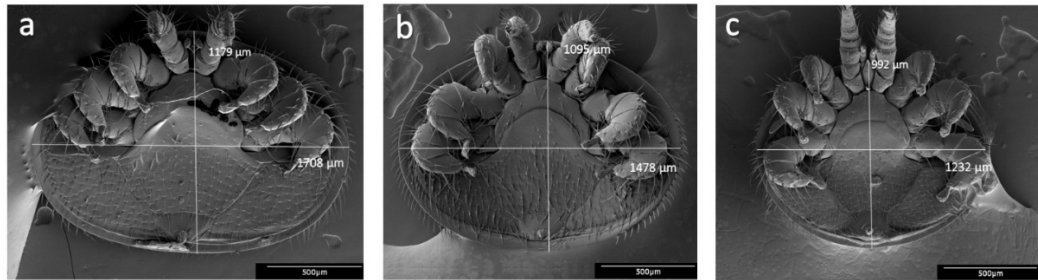


Figure 5.1

Figure 5.1 LT-SEM comparison of two distinct morphotypes and three observed sizes of *Varroa destructor* collected from the same honey bee colony.

a, b, showing typical (**a**), atypical (**c**), intermediate form of *Varroa destructor*. The atypical specimen was substantially smaller than even the smallest recorded specimens of *Varroa jacobsoni*. In addition, it possessed a pentagonally shaped anal plate rather than the typical triangular appearance and a distinct, strongly spiculated cribrum. The intermediate specimen was within the size range of *Varroa jacobsoni* (**b**). All specimens were identified as *Varroa destructor* based on genetic analysis.

The Dorsal Shield

The dorsal region of *V. destructor* is covered by one large convex shield. This shield is covered by numerous pilose setae (Figure 5.2 **a**). These setae are straight at the base and for about half their length before branching for the rest of their length. They bear resemblance to the pilose setae covering their host (Figure 5.2 **b & c**). Most of the setae stand at a nearly 90° angle to the dorsal shield. These setae point away from the body of the mite in the same direction that the ventral setae of the host bee point away from the body of the bee (Figure 5.2 **d**).

Along the margin of the dorsal shield, much thicker, curved setae arise from a row of shallow lateral recesses (Figure 5.2 **a** & **e**). These marginal setae have grooves running their length. Between 18 and 26 marginal setae appear on either side. A row of setae on one side is rarely symmetrical in respect to the other with 23 being the mode on the left side of mites collected for this study and 21 the mode on the right.

Innumerable rows of reticulation form what look like small scales with most having a generally concaved edge. This reticulation comprises the surface of the dorsal shield (Figure 5.3**a**). Like the pilose setae, the reticulation of the of mite closely resembles that of the honey bee (Figure 5.3 **a** & **b**). A conspicuously glabrous region comprises the anterior margin of the dorsal shield (Figure 5.3 **c** & **d**). It is in this area that the reticulation of the dorsum can be seen most clearly.

The shape of the shield itself has utility in the feeding process as well. The convex shape allows for the mite to lift the metasomal plates of the bee like a wedge in order to access their food source, thereby creating a protective feeding chamber. While feeding, the passive quality of their domed shape keeps the plate lifted (Figure 5.3 **e** & **f**).

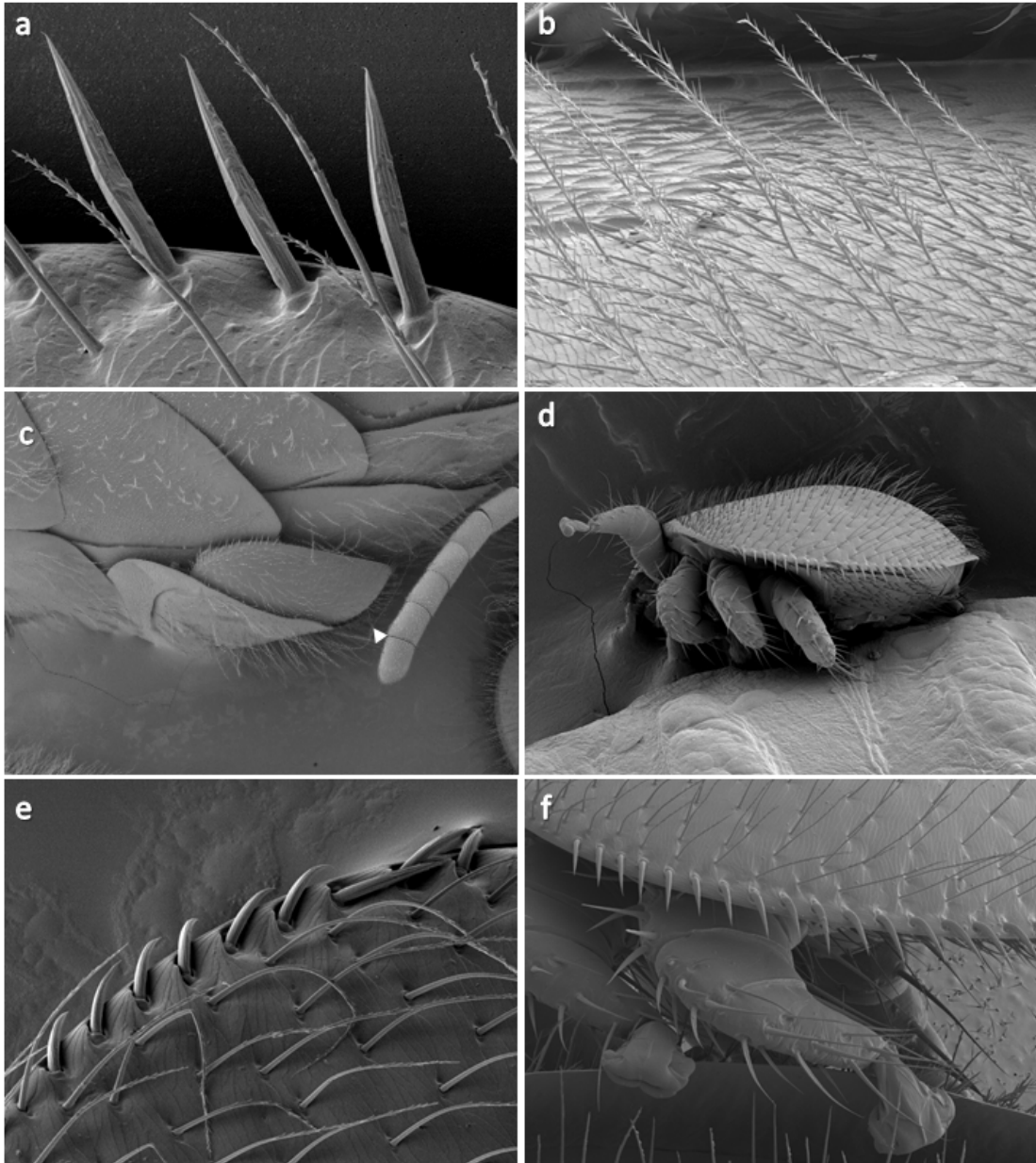


Figure 5.2

Figure 5.2 LT-SEM observation of the setae arising from the dorsal shield of *Varroa destructor*.

a-f showing pilose setae of the dorsum of *Varroa* (**a**) and the venter of a honey bee (**b**). Morphological similarity between them may be an adaptation to establish tactile camouflage to avoid host grooming. *Varroa* feed beneath the ventral sclerites of the honey bee with a portion of their body exposed (**c**). Hairs point away from the body of the mite in the same direction as from the body of the host (**c, d**). Grooved, spine-like setae can also be seen on the edge of the dorsal shield (**a, e, f**).

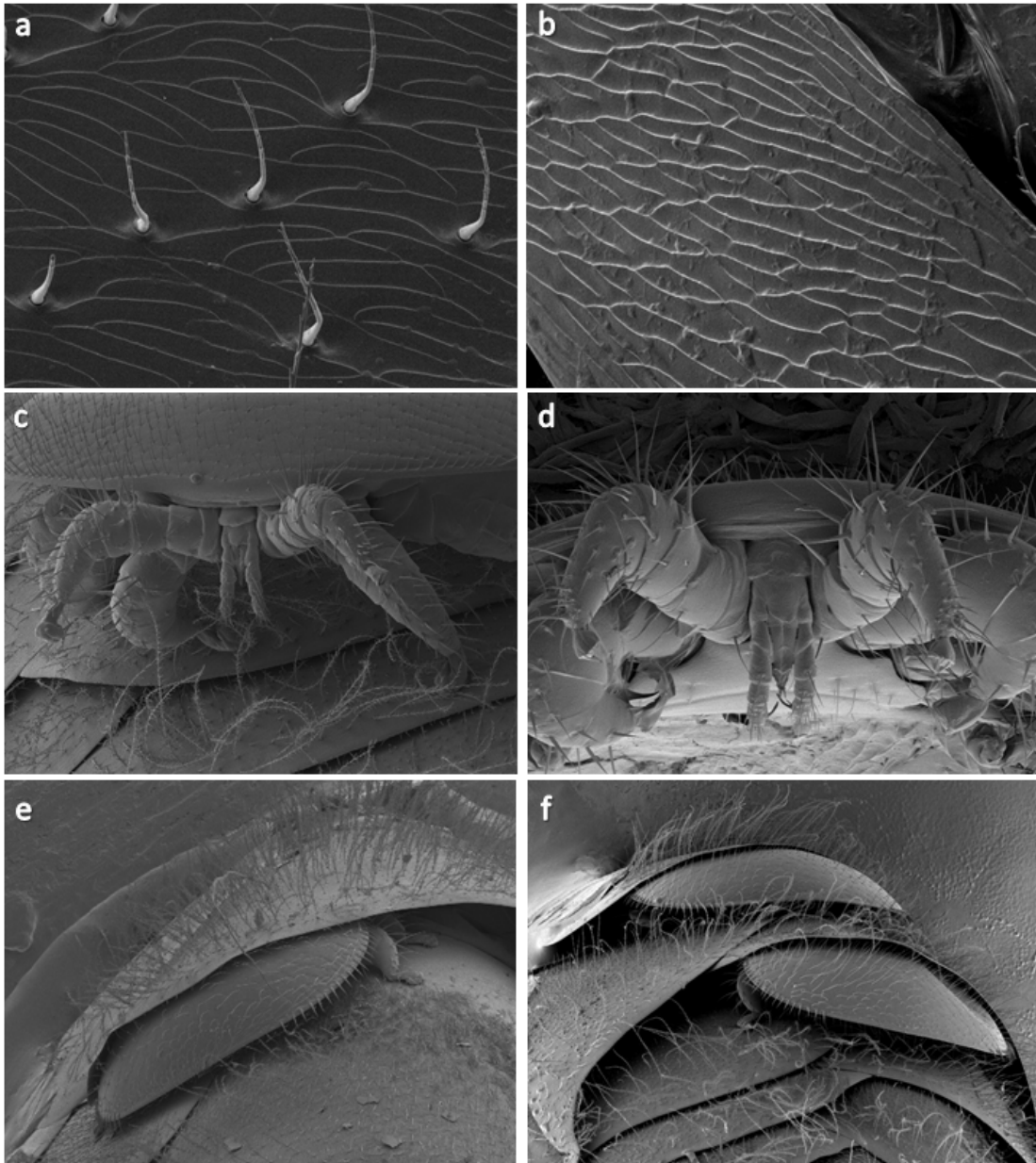


Figure 5.3

Figure 5.3 LT-SEM observation of the fine structure and shape of the dorsal shield of *Varroa destructor*.

a,b showing the reticulation present across the entire surface area of the dorsal shield (**a**). The plates composing the dorsum and venter of the honey bee show very similar reticulation (**b**), likely further adaptation toward tactile camouflage.

c,d showing distinctive glabrous region comprising the anterior margin of the dorsal shield. Reticulation can be observed without being obscured by setae as is the case for the rest of the dorsum.

e,f the domed shape of the dorsal shield allows the parasitic mite to create and passively maintain a feeding chamber on the host bee.

The Ventral Sclerites

The exopodal sclerite is the most anterior sclerite and the most difficult to see as it lies behind the bases of the coxae. Little has been written in description of it. To view it, I removed the legs from multiple specimens. This sclerite has a shape similar to that of a boomerang (Figure 5.4**a**). It runs along the anterior margin of each coxa and comes in contact with the dorsal shield anterior to the gnathosoma. This sclerite shows faint to indiscernible reticulation and is entirely glabrous distinguishing it from the other ventral plates. Reticulation is most recognizable where the exopodal sclerites meets the dorsal shield and becomes more faint as it moves toward the peritrematal shields. Its most anterior margin is difficult to distinguish from the ventral lip of the dorsal shield. Near coxa I, the sclerite begins to separate from the dorsal shield and interscutellar cuticle can be seen between them. Each end of this sclerite merges with the peritrematal shield on the corresponding side of the idiosoma (Figure 5.4**a**).

The sternal sclerite forms a horseshoe-like shape in contact with the coxa of each leg (Figure 5.4 **b** & **c**). This sclerite sits at the base of the camerostome which is formed by the coxae of the first pair of legs and the dorsal shield into which much of the gnathosoma can be retracted. In its retracted state, the sternal sclerite covers the soft perignathosomatic tissue at the base of the gnathosoma and the arthrodistal membrane of

the leg I coxae (Figure 5.4d). This sclerite has varying chaetotaxy. While *V. destructor* is reported to have 10 or 11 some specimens collected in this study have 12 sternal setae (Figure 5.4e).

The genital sclerite has the largest surface area of the ventral sclerites. It has a nearly pentagonal shape with a convex anterior margin. The most anterior region, bordering the sternal sclerite is entirely glabrous and abruptly transitions into being densely hirsute as you move posteriorly. This glabrous region and the largely glabrous anterior metapodal plates create a recognizable division between the prosoma and opisthosoma analogous to the disjugal furrow of the Acariformes. These setae like those of the rest of the venter are simple, unbranched hairs (Figure 5.4f).

To the left and right of the genital sclerite are the anterior and posterior metapodal sclerites. The roughly triangular posterior metapodal sclerites resemble the genital sclerite in being densely hirsute though they are such over their entire surface area. However, the anterior metapodal sclerites are glabrous for most of their surface area with setae present only along the distal margin of the sclerite (Figure 5.4 a & b). The proximal margin of these sclerites conforms to the shape of the 4th coxa. Reticulation near the coxae is stretched laterally to about 2 to 3 times the length of plates elsewhere on the venter. There are fewer than 10 setae (usually 7) on each anterior metapodal sclerite. Many of these features are difficult to observe without removing the 4th pair of legs.

The anal sclerite is triangular in shape with the anus located nearest the lower point of the triangle. The region of the anal sclerite shows a number of variable features. Though typically only 3 setae are present, one on each side of the anus (perianal setae)

and one just beneath it (post-anal), a fourth seta can be found in some specimens near the anterior margin of the plate (Figure 5.5a). Setae periodically arise from the interscutellar membrane but a fourth seta arising from the anal plate itself is unusual. Further variation is found in the region of the cribrum. Most mites collected possessed a barely discernible cribrum with few spicules pointing above the ridges of the rugulose membrane around it (a trait I am referring to as “weakly spiculated”) (Figure 5.5 a-d). Some specimens had a cribrum so weakly spiculated as not to be visible. The only specimen to have a well-defined cribrum was the aforementioned morphologically atypical specimen (Figure 5.5 b & d).

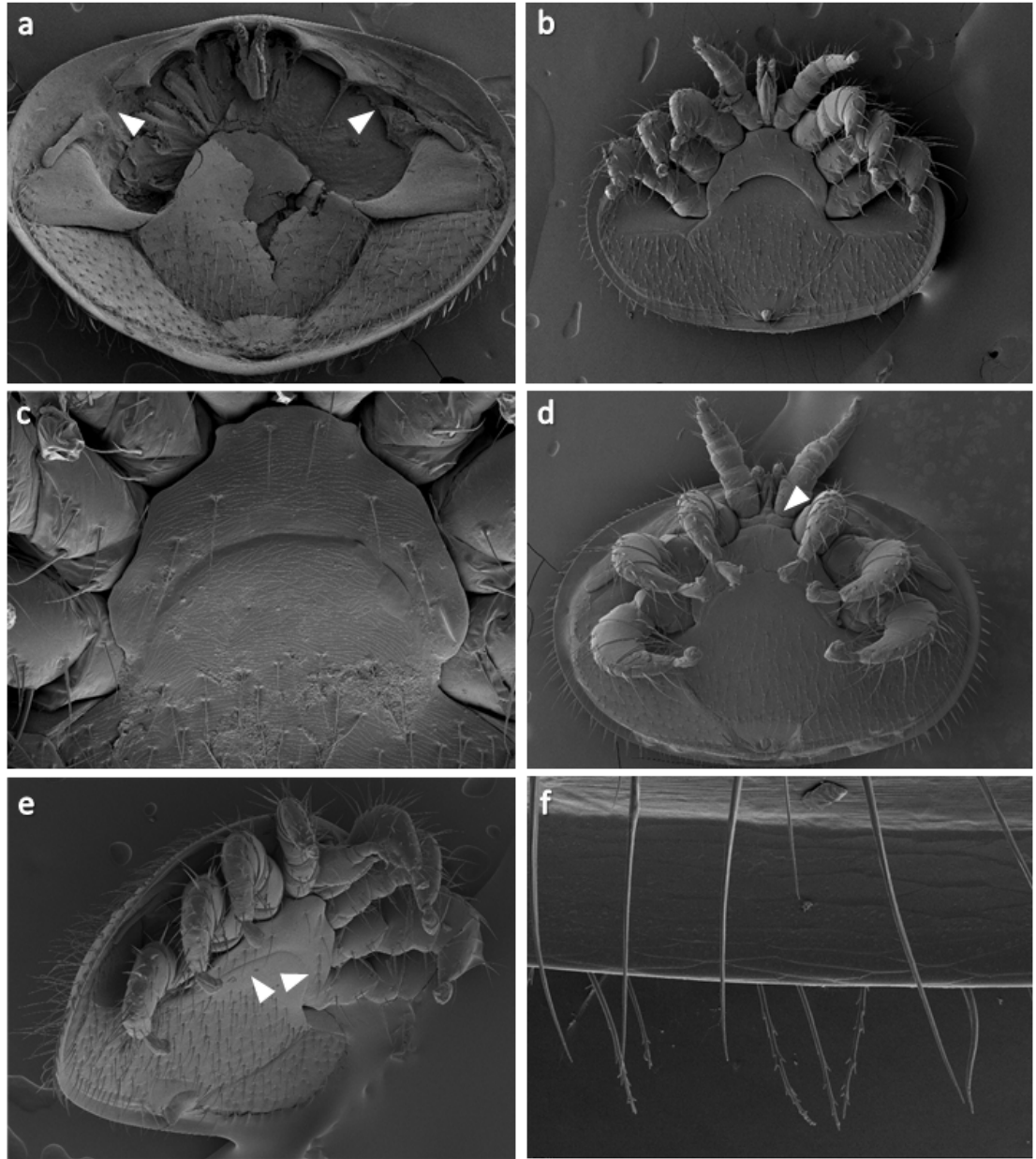


Figure 5.4

Figure 5.4 LT-SEM observation of the fine structure of the ventral sclerites of *Varroa destructor*.

a, legs were removed from a mite to image the exopodal sclerite which sits behind the coxae of the bee. This plate merges with the plates of the peritremes on each side of the mites body. White arrows denote the regions where the exopodal sclerites becomes indistinguishable from the peritrematal shields.

b-e showing the plates that comprise the venter of a *Varroa* female (**b**). Note the variable chaetotaxy on the horseshoe shaped dorsal shield along the margin of the coxae (**b,c,e**). The arthroal membrane normally hidden by the sternal shield is visible sometimes in gravid mites (white arrow).

f showing comparison of setae on the dorsum with those on the venter. Pilose setae, similar in structure to those of the host, are only present on the dorsum. Simple setae, dissimilar from those present on most of the host are hidden on the underside of the mite.

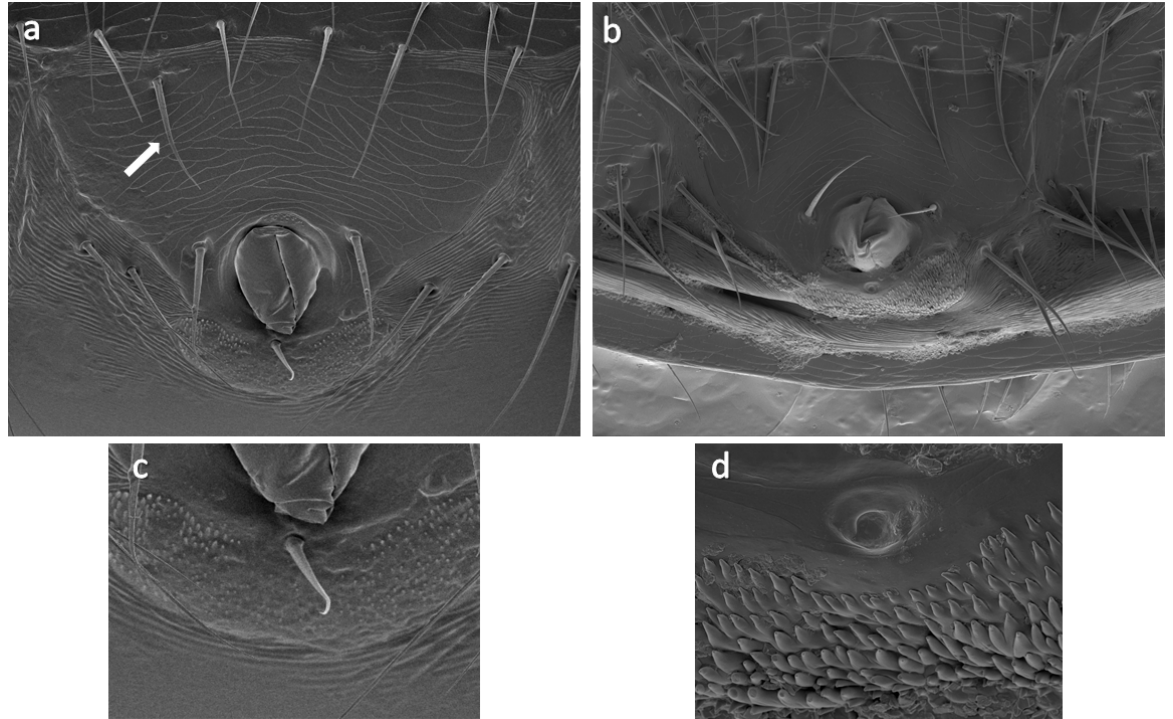


Figure 5.5

Figure 5.5 LT-SEM observations detailing variability in the anal sclerite of *Varroa destructor*.

a-d showing the typical shape of the anal plate (**a**) which forms a triangle with the anus at the lower point of the triangle. Note the one seta arising near the anterior margin of the sclerite (white arrow). The presence of this seta was atypical in our specimens. Image (**b**) details an atypical pentagonally shaped anal sclerite observed in a markedly small individual. Note the differences in shape and spicule definition on the normally crescent shaped cribrum (**a-d**). The specimen in image (**b**) was the only specimen collected with such a distinctive cribrum.

The Gnathosoma

The gnathosoma is a complex of multiple structures including the chelicera, salivary styli, subcapitulum, tritosternum, and palps. To best view these components,

it is often necessary to deconstruct the gnathosoma. When separated it is clear that the opposing fixed digit of the chelicera has been greatly reduced and moved to a lateral position on the proximal face of the mobile digit (Figure 5.6a). On the dorsal surface of the mobile digit are two ax-head shaped teeth. A third less pronounced “tooth” seems apparent at the distal end of the mobile digit but is one of two sensilli present on this section of the digit (with the second just below it). Moving ventrally along the inward facing wall of the mobile digit, the digit thickens forming a ridge (Figure 5.6a & b). When the two chelicera are held closely together they complete a bridge between the two digits (Figure 5.6c & d). The ventral edge of the chelicera curves inward (Figure 5.6a-d). Relatively large salivary stylets are also present on either side of the corniculi. The tips fit into grooves in the lateral faces of the corniculi that likely protect the thin structures from bending or moving too much as they are forced through the integument of the host (Figure 5.6a). A dorsal lyrifissure is present immediately proximal to the mobile digit on the middle article of the chelicera (Figure 5.6a). Posterior to this lyrifissure a flap of tissue called the tectum overhangs the middle article like a visor (Figures 5.3c & d and 5.6a).

The subcapitulum ending in the corniculi forms the ventral face of the gnathosoma. Each corniculus has between 5 & 7 denticles on its ventral surface (Figure 5.6e). In its natural conformation, the corniculi are held together to form a single curved structure. The curved ventral edges of the chelicera fit into this structure pushing together the thickened walls of the inner faces of the chelicera to form a beak-like tube (Figure 5.6c & d). This tube structure appears to be the actual feeding apparatus of the gnathosoma suggesting that these mites feed differently than has been reported

previously. The shape of this tube fits with the feeding wounds inflicted on adult bees (Figure 5.6f). When removed while in contact with the feeding wound, the mouthparts of the mite are still together suggesting that they do not separate while actively feeding as has been posited in previous work.

The tritosternum rests within the subcapitular groove when the gnathosoma is retracted. I observed fine processes of denticles on the inner surface of the subcapitular groove (Figure 5.7a). In addition, I noted a number of corresponding projections on the dorsal surface of the tritosternum that likely engage these processes when fit together. Micropili were present near the base and sometimes more distally along the ventral surface of the tritosternum (Figure 5.7 b & c). These micropili differed in number between 7 and 14.

The palps are typically held with the apotele crossed just below the subcapitulum when the gnathosoma is retracted. These apotele are relatively thick and appear sharp. I noted a variable character on this segment with *V. destructor* sometimes having a small tooth between the long and short claw (Figure 5.7 d & e). The apotele are apparently used as a holdfast when feeding in addition to the ambulacra. Mites feeding through the intersegmental membrane of adult honey bees left an indentation of only the long claw of the ambulacra. Based on the orientation of the long claw, the short claw would be buried in the soft tissue of the host bee. The indentation suggests that the long claw is being used as a brace (Figure 5.7f).

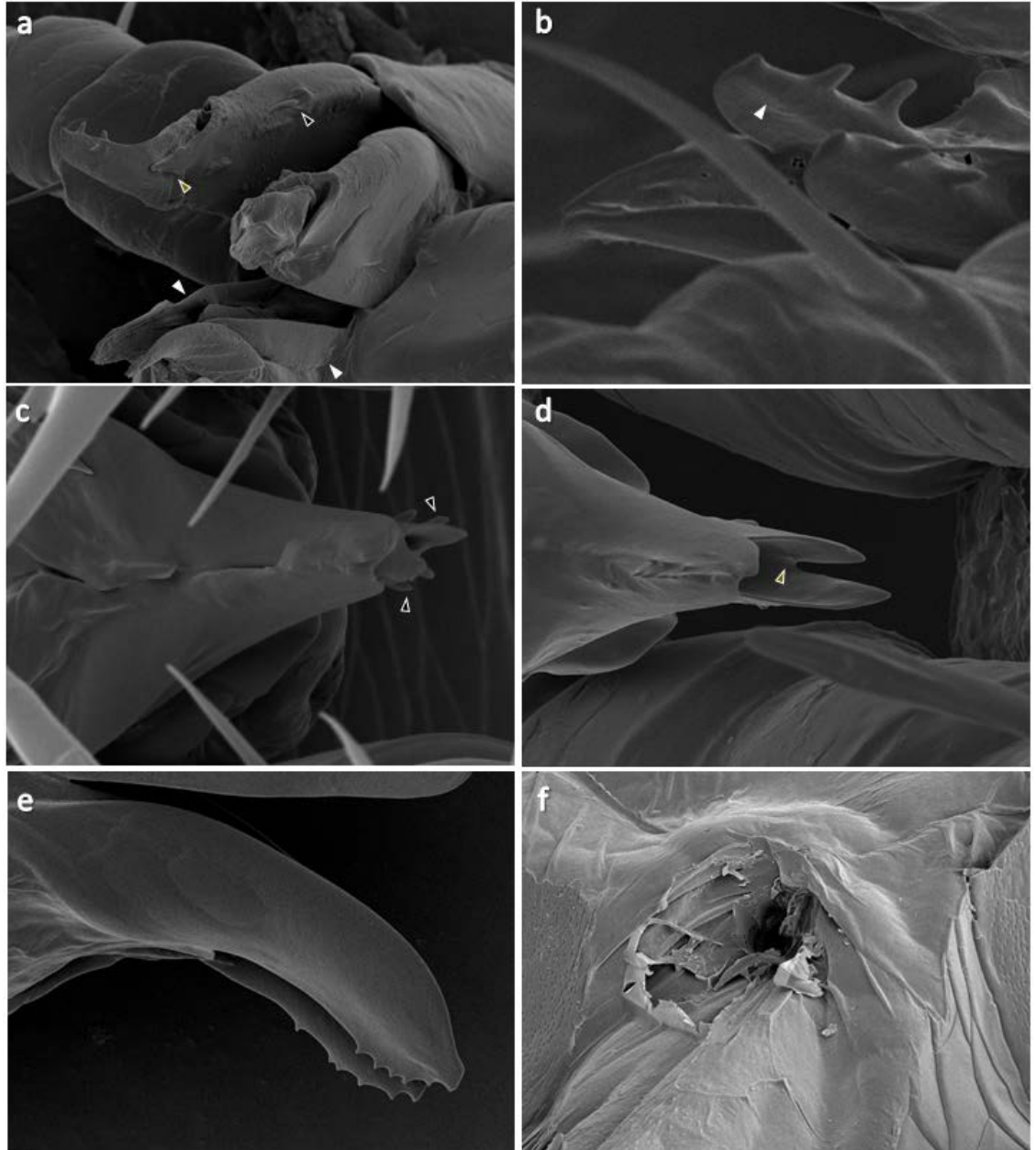


Figure 5.6

Figure 5.6 LT-SEM observations detailing the structuring of the gnathosoma of *Varroa destructor*.

a, gnathosoma was separated from the body of the host dissected to show the complex constitution of this feeding structure. The chelicera arise dorsally with respect to the subcapitulum and corniculus. Well-developed salivary stylets (white arrows) arise on either side of the pre-oral trough and rest along the inner faces of the corniculus for much of their length. The fixed digit of the chelicera, normally similar in size to the mobile digit, has been reduced considerably and moved to a lateral position on the inner face of the mobile digit (brown arrow). A dorsal lyrifissure rests immediately proximal to the mobile digit on the middle article of the chelicera (black arrow).

b-d showing the cheliceral keel present on the inner face of each mobile digit (**b**) (white arrow). The keel on both chelicera can be pushed together to form a ridge (**d**, brown arrow) which seals and forms the roof for the tube-like feeding structure. The teeth along the top of each mobile digit are visible from bottom (**c**) of the chelicera as a result of the angling caused by the cheliceral keels as they are pushed together.

e, corniculi separated from the rest of the gnathosoma. Note the 6 denticles on the ventral edge on both corniculi. This feature varied periodically in specimens between 5 and 7.

f, showing the feeding wound inflicted by *Varroa* on adult an honey bee. Note that the shape of the chelicera when held together as one unit fits with the shape, size and general architecture of the wound.

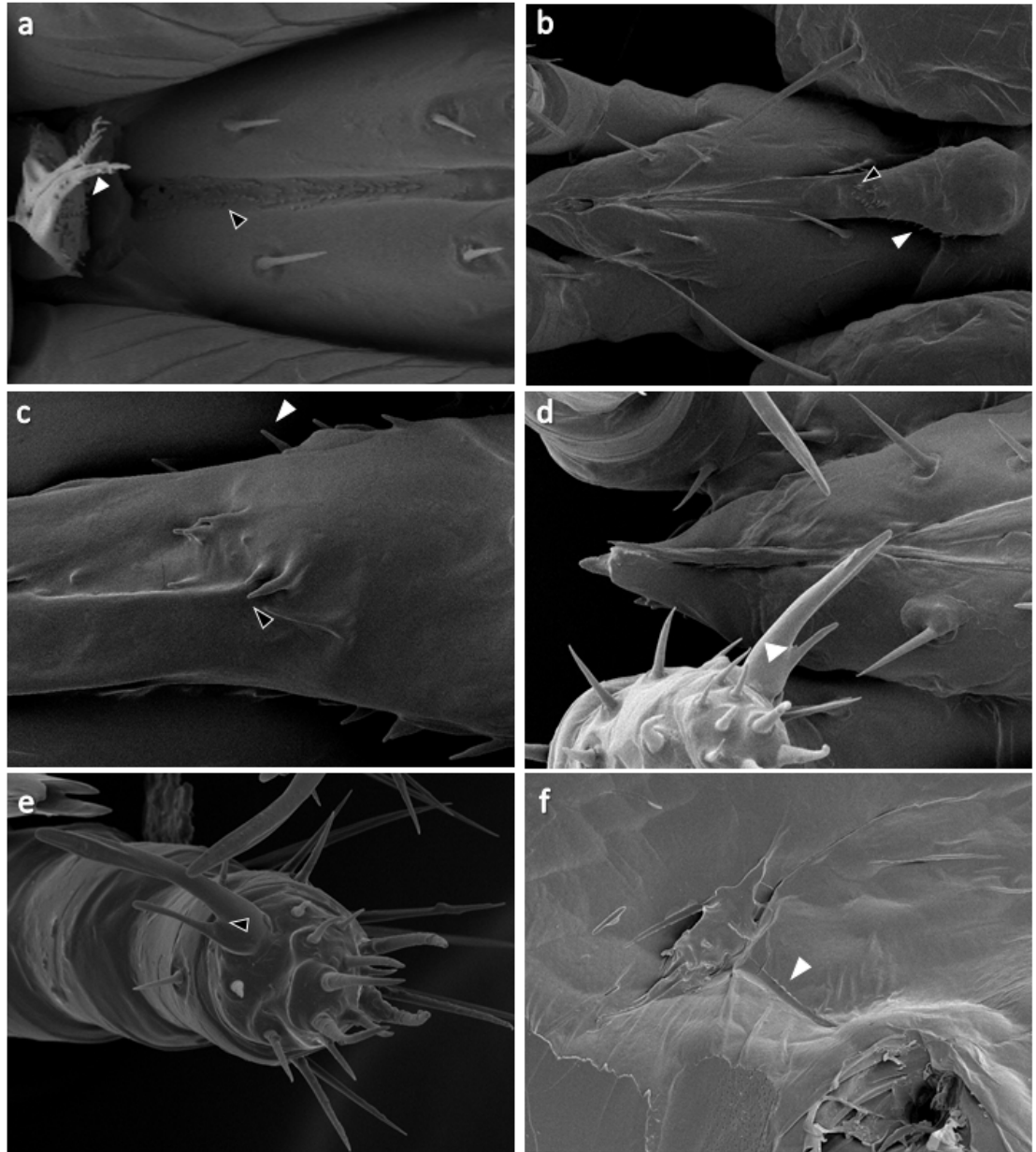


Figure 5.7

Figure 5.7 LT-SEM observations detailing variable structuring of the subcapitular groove, tritosternum and palps of *Varroa destructor*.

a, showing the subcapitular groove with fine, irregularly spaced clusters of denticles populating the inner surface (black arrow). Irregularly spaced rows of denticles also arise from the dorsal surface of the tritosternum likely fitting together with those in the groove forming a process that sieves out any stray particulate matter that may be present in the host meal.

b, c, showing the tritosternum housed in the subcapitular groove (**b, c**). Varying numbers of micropili of unknown (possibly sensory) function arise from the ventral surface of the gnathosoma (black arrows). Between 7 and 14 micropili were present in specimens collected for this study. Note some denticles of the dorsal surface of the tritosternum are visible as well (white arrows).

d, e, the last segment (apotele) of the palp bears a variable character of a small tooth between the large and small claw (**d**, white arrow) in some specimens. Most specimens lacked this trait with a totally smooth region present between the long and short claw (**e**, black arrow).

f, showing the indentation of the palps and gnathosoma of a mite in the intersegmental membrane of an adult host bee. Note the position of the indentation caused by the apotele (white arrow). Only the indentation of the long claw is present. Based on the orientation of the claw pressed against the host membrane the short claw is likely embedded in the membrane to potentially gain leverage to facilitate the gnathosoma piercing the membrane. The long claw appears to be used as a brace against the tissue.

The Legs

For the ambulatory legs (legs II-IV), the femur, genu, and tibia are wider than long (Figure 5.8a). These legs are strongly compressed laterally giving them a flattened appearance (Figures 5.2f & 5.4d). Reticulation on the legs is inconsistent by comparison to the regular patterns on the dorsum and sclerites of the venter. Reticulation can best be seen on the coxae as they arise laterally and become faint or nonexistent dorsally and ventrally (Figure 5.8b). On the remaining leg segments, reticulation is very faint if present at all. The lateral face of on each side of the leg segments is largely glabrous while the dorsal and ventral faces are covered with long acicular setae. These setae originate from a shallow depression and have grooves running their length in the same way as the marginal setae of the dorsum (Figure 5.8f).

Under most natural circumstances, the ambulatory legs are hidden beneath the dorsal shield. Image Figure 5.8c shows why this adaptation is so important as certain genetically distinct populations of honey bees have a proclivity to bite off the apotele of exposed legs on these parasites when grooming. This is likely how the female

imaged above lost both front apotele. When standing, the ambulatory legs are directed posteriorly but the sensory legs are directed anteriorly stretching beyond the dorsal shield leaving them vulnerable to the mandibles of a grooming host (Figure 5.2d & f). However, this image also shows that these mites are more resilient than expected. With the loss of or significant damage to her primary sensory structure, I thought these “ankle-bitten” females would be unable to locate new cells and be effectively removed from the gene pool. To contrary, this specimen was collected from a cell where it was actively reproducing.

The sensory legs have a more cylindrical shape by comparison to the ambulatory legs. A set of relatively short denticles, not previously described in descriptions of *V. destructor*, can be seen projecting from the distal margin of the coxae of the sensory legs (Figure 5.8d & e). Closer inspection of the coxae shows that this process follows the margin of this segment laterally on both sides and dorsally, to some extent, but stops short of the ventral margin (Figure 5.8f). The coxal margin of the ambulatory legs lacks these denticles. Femur to tarsus *V. destructor* have upwards of 10 setae on the dorsal surface of each leg segment. There are substantially fewer hairs on the ventral surface of each leg segment totaling five or fewer on all segments except the tarsus.

The ambulacrum in *V. destructor* is composed of a well-developed paradactylus and a large pulvillus (Figures 5.2f and 5.9a). The shape of the ambulacrum changes substantially when in the raised position and when applied to a surface (compare Figure 5.9a to b and c to d). In addition, I noted the presence of a pair of small setae in an indentation at the base of the apotele (Figure 5.9a, b). These setae flank the

ambulacrum on each of the ambulatory legs but are missing in the sensory legs (Figure 5.9c). Their presence on both sides of the apotele assures that the hairs will be deformed at the full expansion of the ambulacrum suggesting potential sensory, and specifically proprioceptive function, for these setae.

Most mites have substantially diminished ambulacra on the pair of sensory legs but *Varroa* have a well-developed, fully-functional ambulacrum on leg I (Figure 5.9d, f). These ambulacra are used attach to passing bees and to climb onto higher surfaces but also clearly as holdfasts while the mite is feeding on adult host bees. As is shown in Figure 5.9f, the ambulacra hold in place so firmly that when the entire mite is removed, the ambulacra remain securely affixed to the membrane.

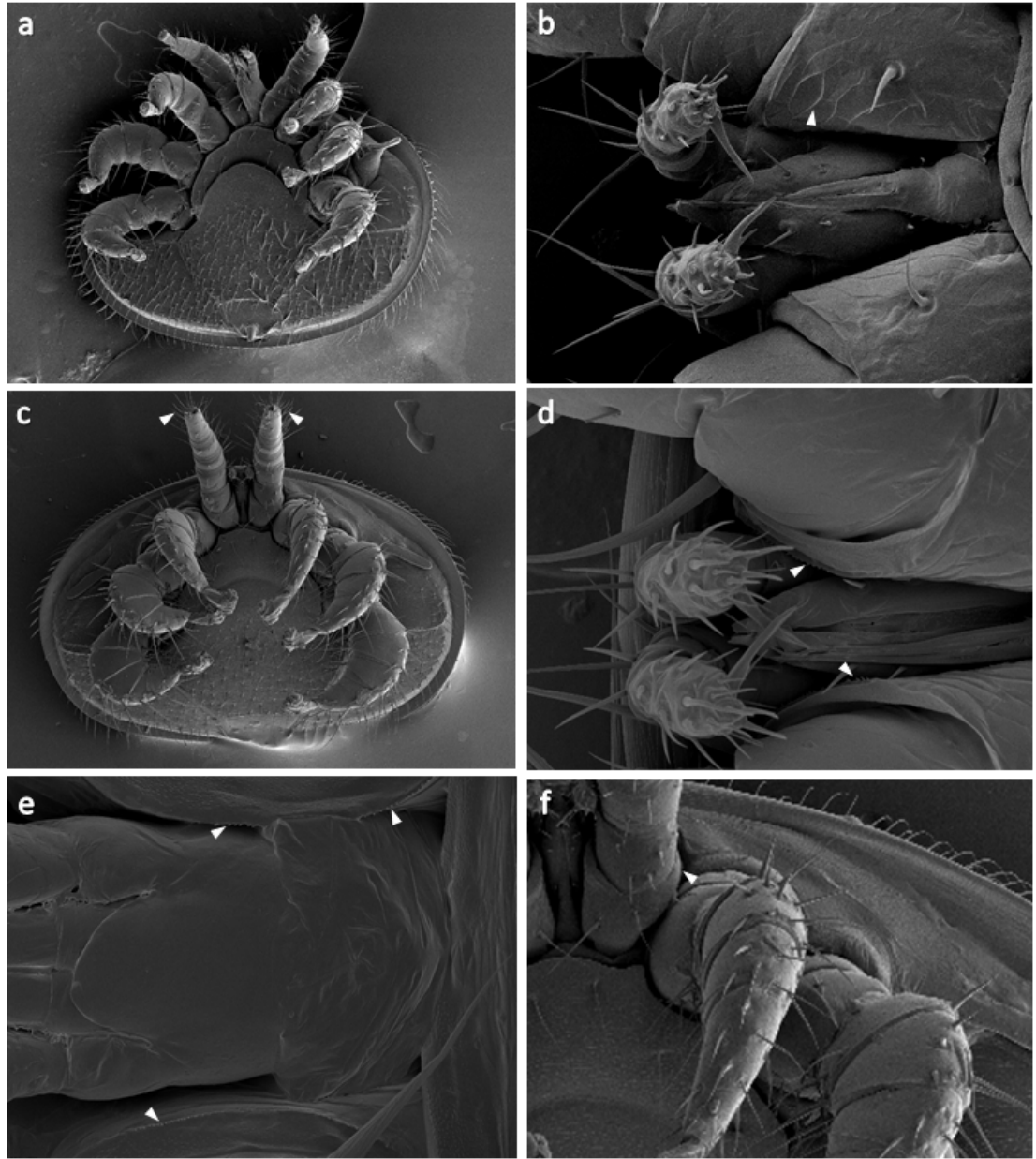


Figure 5.8

Figure 5.8 LT-SEM observations detailing the structure of and characters associated with legs of *Varroa destructor*.

a, showing the legs of *Varroa* which are separated into sensory (leg I) and ambulatory (leg II, III, IV).

b, reticulation clearly visible on the lateral faces of coxae (white arrow) but becomes faint to indistinguishable on the dorsal and ventral surfaces.

c, foundress mite with wounds typical of “ankle biting” genetic line of honey bees. Note, the missing ambulacra from legs I (white arrow). Surprisingly, this mite was still able to find and reproduce normally within a brood cell even with a portion of its primary sensory structure missing.

d-f, showing a fine process of denticles following the distal margin of the coxa of leg I (white arrows). These denticles arise along the lateral edges of the margin and to some extent are present in the region of the coxae behind leg I (**e**).

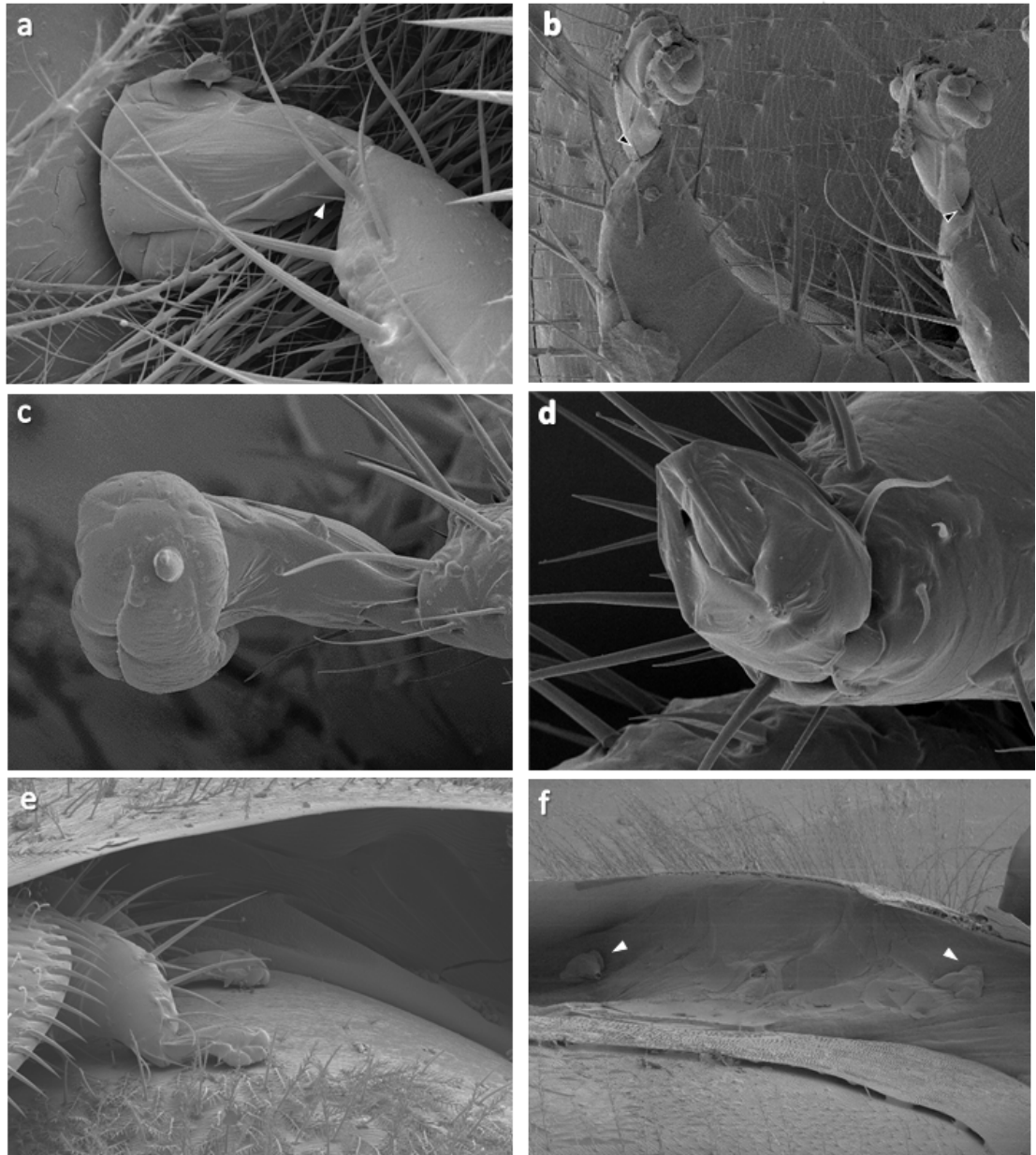


Figure 5.9

Figure 5.9 LT-SEM observations detailing the structure of and characters associated with the ambulacra of *Varroa destructor*.

a, showing an ambulacrum of *Varroa* on an ambulatory leg in its “foot-down” conformation. The shape of the ambulacrum changes noticeably when free or attached to a surface. On each ambulatory leg, a pair of small, likely sensory, setae are present in indentations on either side of the ambulacrum (white arrow). These setae likely function proprioceptively informing the mite of the position of its ambulacrum.

b, ambulacra of ambulatory legs (II and III). Note setae at the base of the ambulacra (black arrows).

c,d, the difference between the free (**c**) and attached (**d**) conformation of the ambulacra on the sensory pair of (leg I) is more pronounced than the difference in the ambulacra of the ambulatory legs. Note the setae on the lateral section of the ambulacrum is not present in the sensory legs.

e,f, showing the ambulacra when attached to an adult honey bee host. The mite is wedged in a pocket of tissue between segments of the bee. The ambulacra of leg I holds especially well to the membrane in this region (**f**). When the mite is removed in a while frozen

The Peritremes

The peritreme runs along a unique pseudo-appendage in *V. destructor* to terminate at the stigma. However, I also noted a slit-like secondary opening just prior to the stigma (Figure 5.10**a** & 5.10**b**). In some specimens, the peritreme terminated at this slit and did not run all the way to the stigma (Figure 5.10**a**). In others, the peritreme intersected this secondary opening crossing directly to the stigma (Figure 5.10**c**). At its resting conformation the peritreme pseudo-appendage fits well with the curved dorsal shield of the mite (Figure 5.10**d** & 5.10**e**). To suit the needs of the mite, the peritremes can also be raised at a nearly 45° angle to the body (Figure 5.10**f**).

Interscutellar cuticle

The intervening space between each ventral sclerite is bridged by the interscutellar cuticle as is the space between the peritremes and the nearest sclerotized

structures. This membrane is distinctly rugulose wherever it arises on the ventral surface of the mite but is especially so around the peritremes (Figure 5.10a). An exception to this observation is found in the case of gravid mites. The state of the developing egg in a gravid female can be reliably determined by how rugulose the membrane appears. Females ready to oviposit or close to this stage have very little, if any, discernible wrinkling in the interscutellar membrane, a fact which is most pronounced in the membrane posterior to the anal plate (Figure 4.2c & 4.2d).

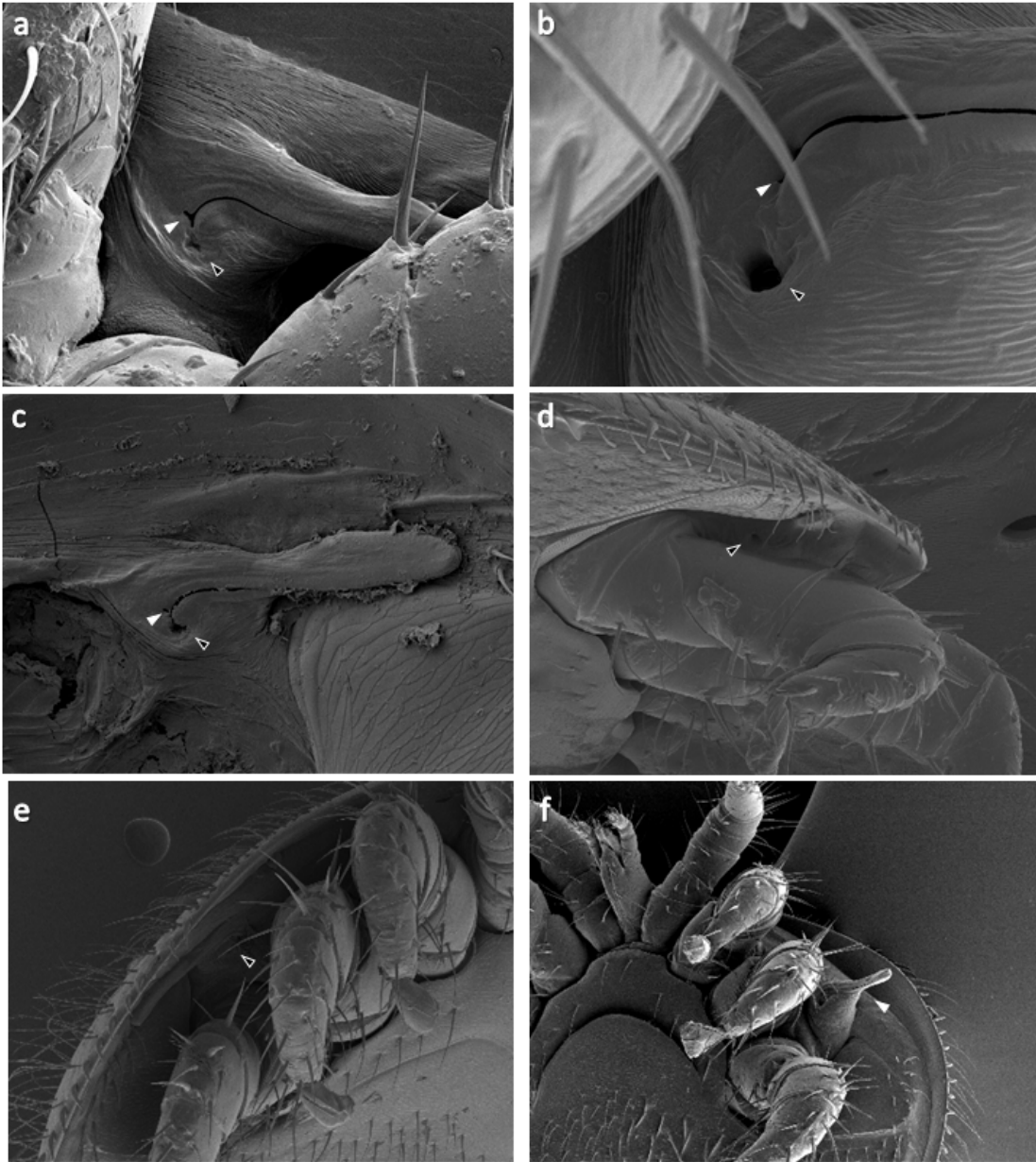


Figure 5.10

Figure 5.10 LT-SEM observations detailing the structure and variability in characters associated with the peritreme and stigma of *Varroa destructor*.

a,b,c showing variation in the terminal point of the peritreme. The peritreme appears to terminate in a slit that runs perpendicular to the path of the rest peritreme (**a,b** white arrows). In most specimens the peritreme terminates in this region and does not connect to the stigma (black arrows). Alternately, in some specimens the peritreme crosses this perpendicular slit and terminates at the stigma (**c**). Note the rugulose intersegmental membrane surrounding the peritreme (**a,b**).

d,e. showing the peritreme when at its resting conformation. This unique pseudo-appendage conforms to the shape of the dorsal shield and leg of the mite.

f, showing raised peritremes apparently characteristic of mites facing respiratory challenge (white arrow). Moving the peritremes can allow the mite to avoid suffocation when submerged in fluid.

Discussion

Several morphological traits showed intraspecific variation. The cribrum was found to be one such character. The character itself seemed to exist on a spectrum between barely discernible (Figure 5.5 **a** & **c**) and well-defined (Figure 5.5 **b** and **d**) with the most defined type represented exclusively by the aforementioned specimen which was morphologically atypical in several respects. Oudemans (1904) (63) described the cribrum normally from his four type specimens of *V. jacobsoni* making no mention of a reduced or barely visible variant. It may have been that his sample size was too small to encompass this trait but in the populations of *V. destructor* I have collected in Asia and in the US, this variant has represented the dominant expression for this trait with only one female collected having a strongly spiculated cribrum. This suggest that the state of the cribrum may be a key morphological difference between species this otherwise cryptic species complex.

Akimov (1985) (111) details even further variation in the cribra of *V. destructor* showing variation I did not observe in this study. In his depictions and descriptions, the spicules of the cribrum are still defined but spread farther apart and populate a much larger area of the anal plate than observed in any of our specimens. He details spicules of the cribrum surrounding the post-anal seta populating the area between the seta and

the anus and in some specimens, reaching up to the margin of the perianal setae on both sides of the anus. Even in our most atypical specimen, the cribrum never reached the perianal setae or the region between the anus and the post-anal seta. Further, variability was observed in the size of the entire body of the mite with the most pronounced variability in the width of the dorsal shield. This may be a response to the selection pressure to keep as much of the body hidden as possible while feeding to avoid being groomed from the host. Ongoing work being conducted by Christmon et al. at the University of Maryland shows that there is now substantial overlap in the size range of *V. destructor* and *V. jacobsoni*.

The most variable character in *V. destructor* appears to be chaetotaxy. The presence and placement of setae on the dorsum and venter of the mite were shown to vary considerably between mites. The number of setae on the margin of the dorsal shield has been noted to vary between 19 and 25 (110, 112) but I found specimens with as few as 18 and one with 26. A fourth simple, and in this instance “pre-anal”, seta sometimes arises on the anal plate showing plasticity in the chaetotaxy of this region as well. This was, however, an infrequent find among samples. The chaetotaxy of the anterior metapodal sclerites and the sternal sclerite varied and the same would likely be found on the genital plate and posterior metapodal sclerites were they not so hirsute to make quantification of differences prohibitively time-consuming. As such, chaetotaxy of much of the venter is likely of limited utility in distinguishing between closely related species like *V. destructor* and *V. jacobsoni*.

The setae of the mite may have limited usefulness in future identification efforts of *Varroa* species but the distribution and structuring of the setae highlight the level of

specialization of this organism for parasitism of honey bees. The pilose hairs of the dorsum are similar in structure to those of their host as is the reticulation of the integument of both organisms. This likely creates a layer of tactile camouflage helping the mite evade grooming, one of the most effective defenses of its original host *Apis cerana* (113). In this host system, there would likely be high selection pressure to develop significant topographical similarity to the host. While looking for physical irregularities on which to focus its grooming efforts, the host bee would likely feel a surface very similar to that of its own integument as it moved from its metasomal plate to the exposed section of the mite feeding just under it. The fact that these hairs arise only from the dorsal shield supports this view as the simple hairs of the venter and the spines of the legs are not exposed to the host.

The structuring of the gnathosoma is markedly atypical for the Dermanyssoidea, specifically the cheliceral-cornicular complex observed in this study. Akimov (1988) (44) hypothesized that the chelicera and corniculi are only held together at rest but when feeding the mite separates these gnathosomal components with the chelicera cutting a larger wound and the subcapitulum sucking food into the pharynx. However, the feeding wounds I observed do not support this position. The feeding wound shows a compact fissure with the distinct downward sloping imprint of the corniculi at the broad base of the wound and curved upper edges with pointed tips likely cut by the teeth of the chelicera. This shape is retained while the mite feeds. If the mite expanded out this complex into its constituent parts while feeding, the shape of this wound would be lost immediately. Further, actively feeding mites when removed from their host still have the cheliceral-cornicular complex together as one structure. These

findings support those of Bautz and Coggins (1992) (114) which suggest that the chelicera form part of the pre-oral trough.

The utility of this apparatus may be entirely mechanical. Together the cheliceral-cornicular complex can exert large force over a relatively small surface area allowing the parasite to more easily pierce the soft membrane of its host. However, the bridge between the two chelicera, which effectively completes a tube, would be unnecessary for this function. It is likely that the tube allows for the production of greater suction. Predigested fatbody would be more viscous than hemolymph and would likely require a more powerful suction to siphon the fluid into the pharynx. It should be noted that siphoning this semi-liquid meal using the chelicera would help to pull food into the pre-oral groove but it would also pull fluid into a blind-ended area above the pre-oral groove which would waste resources were it to remain there. However, ultrathin sections of the gnathosoma photographed by Nuzacci and de Lillo (1995) (105) show that the labrum (a tongue-like structure sitting between the chelicera and the food groove) does not completely fill the space between the paralabra/subcheliceral plates for most of its length. This relatively large cavity on both sides of the labrum would allow for the liquid food to drain into the pre-oral groove beneath it where it can then be siphoned into the pharynx and ingested. This feeding system further evinces the markedly adaptive nature of this mite to its parasitic lifestyle.

Morphological studies conducted previously on the mouthparts of *Varroa* have been undertaken using light microscopy or SEM with critical point drying (40, 42, 105). Collapsing of tissue is clearly visible in images provided by Griffiths (1988) (42). The tectum pulls away from the chelicera creating a large cavity between them apparently

altering their orientation such that they do not fully fit into the subcapitulum. This makes it difficult to discern how the gnathosoma functions as a whole. In our images, the tectum is in direct contact with the proximal dorsal margin of the middle articles of the chelicera maintaining the natural orientation of the gnathosoma.

LT-SEM is an invaluable tool in the study of *Varroa* and clearly minimizes artefacts which alter the appearance of the mites and reduce the quality of data obtained from the resulting images. In future study, I would expect that comparison of these detailed image of *V. destructor* with equally detailed images of *V. jacobsoni* would allow for a more accurate determination of whether there are morphological differences between these species. While I did not have access to *V. jacobsoni*, I was able to collect some *V. destructor* in Asia. There were no significant differences between the populations in the US and those in Asia, however, I had limited access both in the number of colonies sampled in Bangladesh and Thailand and the number of mites collected. Differences may emerge with larger sample size which would provide another tool in better understanding this cryptic species complex.

General Conclusions

Eusocial insect colonies are comprised of a dense aggregation of highly related individuals making a single colony a breeding ground for parasites and disease. Further, protection from predation and the consistent availability of food further increase the attractiveness of eusocial colonies to parasites. The greatest diversity in honey bee species is present in the cavity-nesting species. The evolutionary shift toward cavity-

nesting afforded these organisms nests that could be precisely climate controlled allowing for species like *A. mellifera* to expand their range outside of the tropics (115). However, along with the improvement in nest quality, honey bees heightened the selection pressure on parasites that arrive to develop adaptations necessary to remain in these colonies. Inside the colony, these parasites are immediately afforded an environment with consistently optimal conditions for their reproduction and an environment free of natural enemies. This point illustrated by the far greater diversity of parasites and opportunistic pests present in cavity-nesting honey bee colonies by comparison to the other two sub-genera (i.e. *Micrapis* and *Megapis*) (115, 116). The genus *Varroa* has risen to the occasion becoming one of, if not, the most ubiquitously distributed parasites of honey bees (5, 115, 117, 118). This is clearly due, in no small part, to the multitude of advantageous adaptations described in these studies and several others.

The exploitation of fat body tissue as a trophic resource may be the key adaptation to allow for such successful exploitation of the host. Fat body feeding provides the mites with access to a diverse nutrient profile in the phosphoglycolipoprotein (i.e. vitellogenin). *Varroa* have adapted to feed on honey bees during stages where this tissue is ostensibly at its most nutritionally potent feeding on pupal fat body and that of nurse bees (50, 62, 119). The trophocytes of the fat body absorb the constituent molecules of disintegrating cells in larvae transitioning to the pupal stage and the fat body of nurse bees is characterized by voluminous deposits of vitellogenin (50, 73, 119). Exploitation of fat body in brood likely contributes to the acceleration of developing ova and juvenile mites. Further, the varying adaptations

allowing for this mite to repurpose host reproductive proteins for its own reproductive needs likely further accelerate this process.

Moreover, morphological specializations for parasitism are key to this organism's anatomy. The distribution of setae is a case study in host mimicry with the branched hairs, similar to those of the host, only on the dorsal shield where they can serve to provide the mite with tactile camouflage. The markedly similar reticulation of the integument of the parasite to that of the host likely serves the same purpose. The shape and size of the mite allows for access to a well-protected region while feeding on the adult host and the well-developed footpads ensure the parasite can anchor in place and maintain adequate leverage to force its mouthparts through the soft membrane of the host. The mouthparts of the mite form a feeding structure distinctive in the Dermanyssina and the novelty of the armed peritremes is still not fully understood. The profusion of adaptations in behavior, nutrient acquisition, reproduction, development, and morphology underscore the exceptionally derived nature of this well-suited parasite.

Appendices

Fat Body Function	Associated Pathologies Reported in parasitized <i>A. mellifera</i>
Regulation of Growth & Development/ Facilitation of Metamorphosis (Amdam et al. 2003; Amdam et al. 2004; Mirth et al. 2007; Arrese & Soulages 2010; Stell 2012)	Stunted growth, malformed organs, precocious foraging (Bowen-Walker and Gunn 2001; Amdam et al. 2004; Nilsen et al. 2011; Rosenkrantz et al. 2010)
Nutrient Storage and Mobilization (Keeley 1985; Arrese & Soulages 2010)	Inability to replace and store amino acids; reduction in amino acid and carbohydrate levels (Bowen-Walker 2001; Doormalen 2013)
Pesticide Detoxification (Locke 1980; Landa et al. 1991)	Increased susceptibility to pesticides (Gregorc et al. 2012; Blanken et al. 2015)
Osmoregulation (Keeley 1985; Arrese & Soulages 2010)	Increased water loss and associated weight loss (Bowen-Walker & Gunn 2001; Salvy et al. 2001; Annoscia et al. 2012)
Immune Response (Amdam et al. 2003; Arrese & Soulages 2010)	Decrease in production of antimicrobial peptides (Yang 2005; Yang 2007)
Thermoregulation (Locke 1980; Arrese & Soulages 2010)	Greater overwinter mortality (Sammataro & Needham 1996; Bowen-Walker & Gunn 1998; Amdam et al. 2004)
Regulation of Metabolic Activity (Locke 1980; Keeley 1985; Arrese & Soulages 2010)	Reduction in oxidative phosphorylation & overall metabolic rate (Bowen-Walker & Gunn 2001; vanDoormalen 2013)
Protein & Lipid Synthesis (Locke 1980; Keeley 1985; Arrese & Soulages 2010)	Decrease in lipid and amino acid production (Tewarson 1983; Glinski & Jarosz 1984; Weinberg & Madel 1985; Bowen-Walker & Gunn 2001; Amdam et al. 2004; vanDoormalen et al. 2013)
Vitellogenesis (Amdam et al. 2003; Arrese 2010; Nilsen et al. 2011)	Reduction in vitellogenin titers; decreased lifespan; increased overwinter mortality (Tewarson 1983; Amdam et al. 2003; Amdam et al. 2004)

Table 1

Table 1 detailing the nine primary functions of the fat body and related pathologies associated with *Varroa* feeding. Note that *Varroa* feeding negatively impacts each of the fat body functions.

Bibliography

1. Danforth BN, Sipes S, Fang J, & Brady SG (2006) The history of early bee diversification based on five genes plus morphology. *Proceedings of the National Academy of Sciences* 103(41):15118-15123.
2. Calderone NW (2012) Insect pollinated crops, insect pollinators and US agriculture: trend analysis of aggregate data for the period 1992–2009. *PloS one* 7(5):e37235.
3. Klein A-M, *et al.* (2007) Importance of pollinators in changing landscapes for world crops. *Proceedings of the Royal Society of London B: Biological Sciences* 274(1608):303-313.
4. Meixner MD (2010) A historical review of managed honey bee populations in Europe and the United States and the factors that may affect them. *Journal of invertebrate pathology* 103:S80-S95.
5. Rosenkranz P, Aumeier P, & Ziegelmann B (2010) Biology and control of *Varroa destructor*. *Journal of invertebrate pathology* 103:S96-S119.
6. Committee NHBHSCS (2012) Report on the National Stakeholders Conference on Honey Bee Health. (Alexandria, Virginia. Available: <http://www.usda.gov/documents/ReportHoneyBeeHealth.pdf>).
7. Anderson D & Trueman J (2000) *Varroa jacobsoni* (Acari: Varroidae) is more than one species. *Experimental & applied acarology* 24(3):165-189.
8. Tewarson N, Singh A, & Engels W (1992) Reproduction of *Varroa jacobsoni* in colonies of *Apis cerana indica* under natural and experimental conditions. *Apidologie* 23(2):161-171.
9. Chantawannakul P, De Guzman LI, Li J, & Williams GR (2016) Parasites, pathogens, and pests of honeybees in Asia. *Apidologie* 47(3):301-324.
10. Webster TC & Delaplane KS (2001) *Mites of the honey bee* (Dadant & Sons).
11. de Guzman LI, Rinderer TE, & Stelzer JA (1999) Occurrence of two genotypes of *Varroa jacobsoni* Oud. in North America. *Apidologie* 30(1):31-36.
12. Pimentel D, Zuniga R, & Morrison D (2005) Update on the environmental and economic costs associated with alien-invasive species in the United States. *Ecological economics* 52(3):273-288.
13. Finch DM (2013) GSD Update: Strategies for understanding and controlling species invasions. *October 2013. Albuquerque, NM: US Department of Agriculture, Forest Service, Rocky Mountain Research Station. 9 p.*
14. Le Conte Y, Ellis M, & Ritter W (2010) *Varroa* mites and honey bee health: can *Varroa* explain part of the colony losses? *Apidologie* 41(3):353-363.
15. Shabanov M, Nedyalkov S, & Toshkov A (1978) Varroaosis--a dangerous parasitic disease on bees [caused by the mite *Varroa jacobsoni*]. *American Bee Journal (USA)*.
16. Tewarson NC (1983) *Nutrition and reproduction in the ectoparasitic honey bee (Apis sp.) mite, Varroa jacobsoni* (Eberhard-Karls-Universität Tübingen).

17. Genersch E, *et al.* (2010) The German bee monitoring project: a long term study to understand periodically high winter losses of honey bee colonies. *Apidologie* 41(3):332-352.
18. Aizen MA & Harder LD (2009) The global stock of domesticated honey bees is growing slower than agricultural demand for pollination. *Current biology* 19(11):915-918.
19. Boecking O & Genersch E (2008) Varroosis – the Ongoing Crisis in Bee Keeping. *Journal für Verbraucherschutz und Lebensmittelsicherheit* 3(2):221-228.
20. Neumann P & Carreck NL (2010) Honey bee colony losses. (Taylor & Francis).
21. Glinski Z & Jarosz J (1984) Alterations in haemolymph proteins of drone honey bee larvae parasitized by *Varroa jacobsoni*. *Apidologie* 15(3):329-338.
22. Bowen-Walker PL & Gunn A (2001) The effect of the ectoparasitic mite, *Varroa destructor* on adult worker honeybee (*Apis mellifera*) emergence weights, water, protein, carbohydrate, and lipid levels. *Entomologia Experimentalis et Applicata* 101(3):207-217.
23. Salvy M, *et al.* (2001) Modifications of the cuticular hydrocarbon profile of *Apis mellifera* worker bees in the presence of the ectoparasitic mite *Varroa jacobsoni* in brood cells. *Parasitology* 122(2):145-159.
24. Richards E, Jones B, & Bowman A (2011) Salivary secretions from the honeybee mite, *Varroa destructor*: effects on insect haemocytes and preliminary biochemical characterization. *Parasitology* 138(5):602-608.
25. Annoscia D, Del Piccolo F, & Nazzi F (2012) How does the mite *Varroa destructor* kill the honeybee *Apis mellifera*? Alteration of cuticular hydrocarbons and water loss in infested honeybees. *Journal of insect physiology* 58(12):1548-1555.
26. Van Dooremalen C, *et al.* (2013) Interactive effect of reduced pollen availability and *Varroa destructor* infestation limits growth and protein content of young honey bees. *Journal of insect physiology* 59(4):487-493.
27. Yang X & Cox-Foster DL (2005) Impact of an ectoparasite on the immunity and pathology of an invertebrate: evidence for host immunosuppression and viral amplification. *Proceedings of the National Academy of Sciences of the United States of America* 102(21):7470-7475.
28. Yang X & Cox-Foster D (2007) Effects of parasitization by *Varroa destructor* on survivorship and physiological traits of *Apis mellifera* in correlation with viral incidence and microbial challenge. *Parasitology* 134(3):405-412.
29. Cohen AC (1985) Simple method for rearing the insect predator *Geocoris punctipes* (Heteroptera: Lygaeidae) on a meat diet. *Journal of economic entomology* 78(5):1173-1175.
30. Cohen AC (1989) Ingestion efficiency and protein consumption by a heteropteran predator. *Annals of the Entomological Society of America* 82(4):495-499.
31. Cohen AC (1995) Extra-oral digestion in predaceous terrestrial Arthropoda. *Annual review of entomology* 40(1):85-103.

32. Popel AS, Johnson PC, Kameneva MV, & Wild MA (1994) Capacity for red blood cell aggregation is higher in athletic mammalian species than in sedentary species. *Journal of Applied Physiology* 77(4):1790-1794.
33. Rapp JL (1947) Insect hemolymph: a review. *Journal of the New York Entomological Society* 55(4):295-308.
34. Cohen AC (1998) Solid-to-liquid feeding: the inside (s) story of extra-oral digestion in predaceous Arthropoda. *American Entomologist* 44(2):103-117.
35. Cohen AC (2015) *Insect diets: science and technology* (CRC press).
36. Cohen AC (1998) Biochemical and morphological dynamics and predatory feeding habits in terrestrial Heteroptera. *Predatory Heteroptera: their Ecology and Use in Biological Control*:21-32.
37. Cohen AC & Smith LK (1998) A New Concept in Artificial Diets for *Chrysoperla rufilabris*: The Efficacy of Solid Diets. *Biological Control* 13(1):49-54.
38. Sadvov A (1976) Study of female varroa. *Pchelovodstvo* (8):15-16.
39. Dinda P, Beck I, & Beck M (1977) Some observations on the determination of extracellular fluid volume of jejunal tissue using [3H] inulin and [14C] inulin. *Canadian journal of physiology and pharmacology* 55(3):389-393.
40. Smirnov A (1978) Research results obtained in USSR concerning aetiology, pathogenesis, epizootiology, diagnosis and control of Varroa disease in bees. *Apiacta. An international technical magazine of apicultural and economic information*.
41. Klompen H, Lekveishvili M, & Black WC (2007) Phylogeny of parasitiform mites (Acari) based on rRNA. *Molecular Phylogenetics and Evolution* 43(3):936-951.
42. Griffiths DA (1988) Functional morphology of the mouthparts of *Varroa jacobsoni* and *Tropilaelaps clareae* as a basis for the interpretation of their lifestyles. *Africanized honey bees and bee mites/editors, Glen R. Needham...[et al.]*.
43. Walter DE & Proctor HC (1999) *Mites: ecology, evolution and behaviour* (Springer).
44. Akimov I, Yastrebtsov A, & Gorgol V (1988) Functional and morphological specialization of *Varroa jacobsoni* for parasitism. *Africanized honey bees and bee mites/editors, Glen R. Needham...[et al.]*.
45. Ruijter Ad & Kaas J (1983) anatomy of the Varroa-mite. *Varroa jacobsoni Oud. affecting honey bees: present status and needs: proceedings of a meeting of the EC Experts' Group, Wageningen, 7-9 February 1983/edited by R. Cavalloro*, (Rotterdam: Published for the Commission of the European Communities by AA Balkema, 1983.).
46. Erickson E, Cohen A, & Cameron B (1994) Mite excreta: a new diagnostic for varroasis. *Bee Science* 3:76-78.
47. Arrese EL & Soulages JL (2010) Insect fat body: energy, metabolism, and regulation. *Annual review of entomology* 55:207-225.
48. Cochran DG (1979) URIC ACID ACCUMULATION IN YOUNG AMERICAN COCKROACH NYMPHS. *Entomologia Experimentalis et Applicata* 25(2):153-157.

49. Bolton SJ, Klompen H, Bauchan GR, & Ochoa R (2014) A new genus and species of Nematalycidae (Acari: Endeostigmata). *Journal of Natural History* 48(23-24):1359-1373.
50. Stell I (2012) *Understanding bee anatomy: a full colour guide* (Catford Press).
51. Nichols SW (1989) *Torre-Bueno glossary of entomology* (New York Entomological Society).
52. Lesne P (1896) Mœurs de *Limosina sacra* Meig. (Famille Muscidae, tribu Borborenae). Phenomenes de transport mutuel chez les animaux asticales. Origines de parasitisme chez les insectes Dipteres. *Bull Soc Entomolog Fr* 1627165.
53. Farish D & Axtell R (1971) Phoresy redefined and examined in *Macrocheles muscaedomesticae* (Acarina: Macrochelidae). *Acarologia* 13(1):16-29.
54. Wheeler WM (1919) The phoresy of *Antherophagus*. *Psyche* 26(6):145-152.
55. Sabelis MW & Bruin J (2010) *Trends in acarology: proceedings of the 12th international congress* (Springer Science & Business Media).
56. Floate KD (2011) Arthropods in cattle dung on Canada's grasslands. *Arthropods of Canadian grasslands* 2:71-88.
57. Revainera P, Lucia M, Abrahamovich AH, & Maggi M (2014) Spatial aggregation of phoretic mites on *Bombus atratus* and *Bombus opifex* (Hymenoptera: Apidae) in Argentina. *Apidologie* 45(5):579-589.
58. Reynolds DR, Reynolds AM, & Chapman JW (2014) Non-volant modes of migration in terrestrial arthropods. *Animal Migration* 2(1).
59. Kanbar G & Engels W (2003) Ultrastructure and bacterial infection of wounds in honey bee (*Apis mellifera*) pupae punctured by *Varroa* mites. *Parasitology Research* 90(5):349-354.
60. Polak M (1996) Ectoparasitic Effects on Host Survival and Reproduction: The *Drosophila*--*Macrocheles* Association. *Ecology* 77(5):1379-1389.
61. Camerik A (2010) Phoresy revisited. *Trends in Acarology*, (Springer), pp 333-336.
62. Xie X, Huang ZY, & Zeng Z (2016) Why do *Varroa* mites prefer nurse bees? *Scientific reports* 6:28228.
63. Oudemans AC (1904) On a new genus and species of parasitic acari. *Notes from the Leyden Museum* 24(4):216-222.
64. Beetsma J, Boot WJ, & Calis J (1999) Invasion behaviour of *Varroa jacobsoni* Oud.: from bees into brood cells. *Apidologie* 30(2-3):125-140.
65. Garedew A, Schmolz E, & Lamprecht I (2004) The energy and nutritional demand of the parasitic life of the mite *Varroa destructor*. *Apidologie* 35(4):419-430.
66. Keeley LL (1985) Physiology and biochemistry of the fat body. *Comprehensive insect physiology, biochemistry and pharmacology* 3:211-248.
67. Locke M (1980) The cell biology of fat body development. *Insect Biology in the Future*, (Elsevier), pp 227-252.
68. Roma GC, Bueno OC, & Camargo-Mathias MI (2010) Morpho-physiological analysis of the insect fat body: a review. *Micron* 41(5):395-401.
69. Weinberg K & Madel G (1985) The influence of the mite *Varroa jacobsoni* Oud. on the protein concentration and the haemolymph volume of the brood

- of worker bees and drones of the honey bee *Apis mellifera* L. *Apidologie* 16(4):421-436.
70. Bruce W, Chiesa F, Marchetti S, & Griffiths D (1988) Laboratory feeding of *Varroa jacobsoni* Oudemans on natural and artificial diets (Acari: Varroidae). *Apidologie* 19(2):209-218.
 71. Rosenkranz P & Engels W (1994) Infertility of *Varroa jacobsoni* females after invasion into *Apis mellifera* worker brood as a tolerance factor against varroaosis. *Apidologie* 25(4):402-411.
 72. Dietemann V, *et al.* (2013) Standard methods for varroa research. *Journal of apicultural research* 52(1):1-54.
 73. Amdam GV, Norberg K, Hagen A, & Omholt SW (2003) Social exploitation of vitellogenin. *Proceedings of the national academy of sciences* 100(4):1799-1802.
 74. Amdam GV, Hartfelder K, Norberg K, Hagen A, & Omholt SW (2004) Altered physiology in worker honey bees (Hymenoptera: Apidae) infested with the mite *Varroa destructor* (Acari: Varroidae): a factor in colony loss during overwintering? *Journal of Economic Entomology* 97(3):741-747.
 75. Blanken LJ, van Langevelde F, & van Dooremalen C (2015) Interaction between *Varroa destructor* and imidacloprid reduces flight capacity of honeybees. *Proceedings of the Royal Society B: Biological Sciences* 282(1820):20151738.
 76. Landa V, Sula J, Marec F, Matha V, & Soldan T (1991) Methods for assessing exposure of insects. *Methods for assessing exposure of human and non-human biota*, Edited by Tardiff R. G., Goldstein B., Published by John Wiley & Sons Lid.
 77. Bailey L & Ball B (1991) Honey bee pathology. *Honey bee pathology*. (Ed. 2).
 78. Annoscia D, *et al.* (2018) Haemolymph removal by the parasite *Varroa destructor* can trigger the proliferation of the Deformed Wing Virus in mite infested bees (*Apis mellifera*), contributing to enhanced pathogen virulence. *bioRxiv*:257667.
 79. Alberti G & Zeck-Kapp G (1986) The nutritive egg development of the mite, *Varroa jacobsoni* (Acari, Arachnida), an ectoparasite of honey bees. *Acta Zoologica* 67(1):11-25.
 80. Rosenkranz P, *et al.* (1993) Juvenile hormone titer and reproduction of *Varroa jacobsoni* in capped brood stages of *Apis cerana indica* in comparison to *Apis mellifera ligustica*. *Apidologie* 24(4):375-382.
 81. Steiner J, Diehl PA, & Vlimant M (1995) Vitellogenesis in *Varroa jacobsoni*, a parasite of honey bees. *Experimental & applied acarology* 19(7):411-422.
 82. Dittmann F & Steiner J (1997) Intercellular connection between the lyrate organ and the growing oocyte in *Varroa jacobsoni* as revealed by Lucifer Yellow dye-coupling. *Journal of apicultural research* 36(3-4):145-149.
 83. Ifantidis M (1997) Ontogenesis of *Varroa jacobsoni* Oud. *Cahiers Options Méditerranéennes. Varroosis in the Mediterranean region. CIHEAM, Zaragoza, ES*. p:13-21.

84. Cabrera Cordon A, Shirk P, Duehl A, Evans J, & Teal P (2013) Variable induction of vitellogenin genes in the varroa mite, *Varroa destructor* (Anderson & Trueman), by the honeybee, *Apis mellifera* L, host and its environment. *Insect molecular biology* 22(1):88-103.
85. Frey E, Odemer R, Blum T, & Rosenkranz P (2013) Activation and interruption of the reproduction of *Varroa destructor* is triggered by host signals (*Apis mellifera*). *Journal of invertebrate pathology* 113(1):56-62.
86. Trouiller J & Milani N (1999) Stimulation of *Varroa jacobsoni* Oud. oviposition with semiochemicals from honeybee brood. *Apidologie* 30(1):3-12.
87. Tewarson NC & Engels W (1982) Undigested uptake of non-host proteins by *Varroa jacobsoni*. *Journal of Apicultural Research* 21(4):222-225.
88. Havukainen H, Halskau Ø, Skjaerven L, Smedal B, & Amdam GV (2011) Deconstructing honeybee vitellogenin: novel 40 kDa fragment assigned to its N terminus. *Journal of Experimental Biology* 214(4):582-592.
89. Nogge G & Giannetti M (1979) Midgut absorption of undigested albumin and other proteins by tsetse, *Glossina m. morsitans* (Diptera: Glossinidae). *Journal of medical entomology* 16(3):263-263.
90. Walker MD & Rotherham ID (2010) The common swift louse fly, *Crataerina pallida*: An ideal species for studying host-parasite interactions. *Journal of Insect Science* 10(1).
91. Ackerman S, Clare FB, McGill T, & Sonenshine DE (1981) Passage of host serum components, including antibody, across the digestive tract of *Dermacentor variabilis* (Say). *The Journal of parasitology* 67(5):737-740.
92. Sammataro D & Needham GR (1996) Developing an integrated pest management (IPM) scheme for managing parasitic bee mites. *American bee journal*.
93. Bowen-Walker P & Gunn A (1998) Inter-host transfer and survival of *Varroa jacobsoni* under simulated and natural winter conditions. *Journal of apicultural research* 37(3):199-204.
94. Kent C, Issa A, Bunting A, & Zayed A (2011) Evolution of vitellogenin, a gene with roles in honeybee social behaviors. *Genes, Brain and Behavior* 10(4):510.
95. Salmela H, *et al.* (2016) Ancient duplications have led to functional divergence of vitellogenin-like genes potentially involved in inflammation and oxidative stress in honey bees. *Genome biology and evolution* 8(3):495-506.
96. Ochoa R, Pettis JS, Erbe E, & Wergin WP (2005) Observations on the honey bee tracheal mite *Acarapis woodi* (Acari: Tarsonemidae) using low-temperature scanning electron microscopy. *Experimental & applied acarology* 35(3):239-249.
97. de Guzman L, Williams G, Khongphinitbunjong K, & Chantawannakul P (2017) Ecology, Life History, and Management of *Tropilaelaps* Mites. *Journal of economic entomology* 110(2):319.
98. Mossadegh M (1990) Development of *Euvarroa sinhai* (Acarina: Mesostigmata), a parasitic mite of *Apis florea*, on *A. mellifera* worker brood. *Experimental & applied acarology* 9(1-2):73-78.

99. Mossadegh M (1990) In Vitro Observations on Ontogenesis of the Mite, Euvarroa Sinhai Delfinado & Baker (Acari: Varroidae), in Drone Brood Cells of the Honeybee, Apis Mellifera L. *Journal of Apicultural Research* 29(4):230-232.
100. Poliakov A, Smirnov A, Kulikovskii A, & Smirnova O (1975) Study of the Varroa jacobsoni mite. *Pchelovodstvo*.
101. Liu T (1982) A scanning electron microscope study on the female mite Varroa jacobsoni (Oudemans, 1904)[Honeybee pest, morphology]. *American Bee Journal*.
102. De Ruijter A & Kaas J (1983) The anatomy of the Varroa mite. *Varroa jacobsoni oud affecting honey bees: present status and needs. AA Balkema, Rotterdam*:45-47.
103. Styer W (1983) Mites of honeybees as seen by scanning electron microscope (SEM)[Acari, Apis mellifera, infestations]. *American Bee Journal*.
104. de Lillo E, Di Palma A, & Nuzzaci G (2001) Morphological adaptations of mite chelicerae to different trophic activities (Acari). *Entomologica* 35:125-180.
105. Nuzzaci G & de Lillo E (1995) Functional morphology of the mouthparts of Varroa jacobsoni Oudemans female (Acari: Varroidae). *The Acari—physiological and ecological aspects of Acari–host relationships. Warszawa: Dabor. p*:79-89.
106. Nuzzaci G, de Lillo E, & Porcelli F (2016) Functional morphology of the mouthpart sensilla in females of Varroa jacobsoni Oudemans (Acari: Varroidae). *Entomologica* 27:41-67.
107. Craig S & Beaton CD (1996) A simple cryo-SEM method for delicate plant tissues. *Journal of Microscopy* 182(2):102-105.
108. Katsen-Globa A, Puetz N, Gepp MM, Neubauer JC, & Zimmermann H (2016) Study of SEM preparation artefacts with correlative microscopy: Cell shrinkage of adherent cells by HMDS-drying. *Scanning* 38(6):625-633.
109. De Guzman L, Rinderer T, & Stelzer J (1997) DNA evidence of the origin of Varroa jacobsoni Oudemans in the Americas. *Biochemical genetics* 35(9-10):327-335.
110. de Guzman LI & Rinderer TE (1999) Identification and comparison of Varroa species infesting honey bees. *Apidologie* 30(2-3):85-95.
111. Akimov I & Yastrebtsov A (1985) Variability of some characters of the mite Varroa jacobsoni Oudemans, 1904—a parasite of the honey bee. *Dokl Akad Nauk USSR Biol Nauki* 9:58-60.
112. Fernandez N & Coineau Y (2006) *Varroa: The Serial Bee Killer Mite: to be Able to Combat Her, One Must Properly Understand Her* (Atlantica).
113. Büchler R, Drescher W, & Tornier I (1992) Grooming behaviour of Apis cerana, Apis mellifera and Apis dorsata and its effect on the parasitic mites Varroa jacobsoni and Tropilaelaps clareae. *Experimental & applied acarology* 16(4):313-319.
114. Bautz RA & Coggins JR (1992) Scanning Electron Microscopy of Female Varroa jacobsoni (Arthropoda: Acarina), Ectoparasite of the Honeybee Apis mellifera. *Transactions of the American Microscopical Society*:28-35.

115. Hepburn HR & Radloff SE (2011) *Honeybees of Asia* (Springer Science & Business Media).
116. Oldroyd BP & Wongsiri S (2009) *Asian honey bees: biology, conservation, and human interactions* (Harvard University Press).
117. Sammataro D, Gerson U, & Needham G (2000) Parasitic mites of honey bees: life history, implications, and impact. *Annual review of entomology* 45(1):519-548.
118. Zhang Z-q (2000) Notes on Varroa destructor (Acari: Varroidae) parasitic on honeybees in New Zealand. *Systematic and Applied Acarology Special Publications* 5(1):9-14.
119. Toth AL & Robinson GE (2005) Worker nutrition and division of labour in honeybees. *Animal behaviour* 69(2):427-435.